decrease in PBN-adduct concentration by ascorbic acid was not an artefact associated with adduct instability and subsequent reduction to an EPR "silent" hydroxylamine.
These findings suggest that PBN-trapped free radicals detected following human exercise are likely derived from the oxidation of polyunsaturated fatty acid membranes. Furthermore, clear ex vivo and in vitro evidence suggests that ascorbic acid is an effective antioxidant when required to terminate lipid peroxidation and inhibit the generation of oxygen-centred alkoxyl radicals.

Davison GW et al. (2006). Clin Sci 110, 133-141.

Authors have confirmed where relevant, that experiments on animals and man were conducted in accordance with national and/or local ethical requirements.

C16

Heat shock and antioxidant protein adaptations of human skeletal muscle to high intensity interval running training: a comparison of the vastus lateralis and gastrocnemius muscle

J.P. Morton[1], J.D. Bartlett[1], L. Croft[1], D.P. MacLaren[1], T. Reilly[1], A. McArdle[2] and B. Drust[1]

[1]Research Institute for Sport and Exercise Sciences, Liverpool John Moores University, Liverpool, UK and [2]School of Clinical Sciences, University of Liverpool, Liverpool, UK

Skeletal muscle adapts to the stress of acute (Morton et al., 2006) and chronic (Morton et al., in press) exercise via increased content of heat shock proteins (HSPs) and antioxidant defences. An increased content of such defences following stress function to restore cellular homeostasis and to protect the cell from further insults. A consistent elevation of 'stress proteins' during training may therefore be a crucial component of the cellular mechanisms by which regular exercise provides protection against exercise-induced muscle damage. Adaptations of HSPs and antioxidants following running exercise have only been studied in the vastus lateralis, despite the gastrocnemius muscle being more metabolically active in this exercise mode(Costill et al., 1974). The aim of this study was to compare HSP and antioxidant adaptations in the vastus lateralis and gastrocnemius following high intensity interval training.
Eight males performed 50 min of high intensity intermittent running exercise, four times per week for six weeks. The protocol consisted of five 3 min bouts at 90% 2max separated by 3 min active recovery periods (1.5 min at 25% 2max followed by 1.5 min at 50% 2max). A 10 min warm-up and cool down period at 70% 2max was also performed. Assessments of 2max, running economy (RE) and performance on a Yo-Yo intermittent recovery 2 test (IRT2) were performed before and after training. Resting muscle biopsies were obtained from the lateral portion of the gastrocnemius and from the mid-portion of the vastus lateralis muscle pre- and post-training. Training induced significant ($P<0.05$) improvements in 2max (10%), RE (4%) and IRT2 (16%). Training resulted in significant increases ($P<0.05$) in HSP60 (22%), αB-crystallin (52%), MnSOD (38%) and a tendency ($P<0.09$) for an increase in HSP70 (20%) content of the gastrocnemius. In contrast, only αB-crystallin (22%) and MnSOD (37%) significantly increased ($P<0.05$) in the vastus lateralis following training. HSP27 was unchanged in either muscle following training.
This study is the first to examine HSP and antioxidant protein adaptations of the gastrocnemius and vastus lateralis muscle to exercise. Data demonstrate that short-term high intensity intermittent exercise induces a more pronounced up-regulation of stress proteins in the gastrocnemius muscle compared with the vastus lateralis. This differential response between muscles is likely due to differences in recruitment patterns (and hence greater activation of associated signalling pathways) during this mode of exercise. We therefore suggest that the gastrocnemius muscle is a more suitable muscle for which to study the exercise-induced stress response of human skeletal muscle during running.

Costill D et al (1974). Acta Physiol Scand 91, 475-481.

Morton JP et al (2006). J Appl Physiol 101, 176-182.

Morton JP et al (in press). Med Sci Sports Exer.

Supported by a research grant from GlaxoSmithkline Consumer Healthcare (UK)

Authors have confirmed where relevant, that experiments on animals and man were conducted in accordance with national and/or local ethical requirements.

C17

Exercise-induced cardiac stem cell activation and ensuing myocyte hyperplasia contribute to left ventricular remodelling

G.M. Ellison[1], C. Vicinanza[2], I. Mendicino[2], W. Sacco[2], S. Purushothaman[1], C. Indolfi[2], D.F. Goldspink[1], B. Nadal-Ginard[3] and D. Torella[1,2]

[1]Stem Cell and Molecular Physiology Laboratory, Research Institute for Sport and Exercise Sciences, Liverpool JM University, Liverpool, UK, [2]Molecular and Cellular Cardiology Laboratory, Department of Medicine, Magna Graecia University, Catanzaro, Italy and [3]Heart Regeneration Studies, Coretherapix, Madrid, Spain

Traditionally, it was thought that exercise improved cardiac function by only increasing myocardial mass and contractility through physiological hypertrophy of existing myocytes. Recent data on myocardial cell homeostasis and the identification of cardiac stem cells (CSCs), in the adult mammalian heart, could challenge this concept. We sought to assess if CSC activation and ensuing myocyte formation participates in cardiac remodeling induced by exercise. To this aim, 36 FVB mice underwent a programme of controlled swimming exercise (Ex) and were sacrificed at different time points over 28 days. Ten untrained mice acted as sedentary controls (Sed). To track myocardial proliferation, BrdU was administered (i.p.) twice daily. Hearts were processed for immunohistochemistry and confocal microscopy analysis (n=30) and c-kit-positive CSCs and myocytes were also isolated for molecular analyses (n=16). Results showed that exercise training resulted in increased heart:body weight ratios in Ex (6.1±0.7mg/g, Mean±SD) vs. Sed (4.3±0.2mg/g) mice. Average myocyte volume was greater in

Ex mice, compared to Sed. The distribution of myocyte sizes showed the presence of both larger (hypertrophied) and smaller myocytes in the ventricular wall of the Ex vs. Sed hearts. To address the source of these smaller myocytes, we evaluated CSC myocardial activation. The number of CSCs increased 5-fold in the ventricular wall of the Ex vs. Sed mice. Most CSCs were proliferating (BrdU and/or Ki-67 positive) and many expressed the cardiac transcription factor, GATA-4, representing cardiac progenitors. Small amounts of sarcomeric proteins were found in the cytoplasm of some of these cells, corresponding to myocyte precursors. Consequently, we detected increased numbers of small BrdU (3±1%) and Ki-67 (1.3±0.1%) positive myocytes in Ex vs. Sed (BrdU=0.03±0.01%;Ki-67=0.01±0.01%) hearts. These cells were transiently cell cycle competent as shown by their expression of p107 instead of pRB, followed by E2F1 and c-myc. Also, Cyclin E/cdk2 and Cyclin B1/cdc2 complexes were increased in the small myocytes isolated from Ex mice. IGF-1 expression progressively increased in myocytes, and then in CSCs, over 28 days of exercise training. This increased IGF-1 expression resulted in a higher number of CSCs, through IGF-1R activation and Akt phosphorylation in CSCs, isolated from Ex compared to Sed mice. This demonstrates that the IGF-1Rs are functional and signal to their downstream physiological targets in the activated CSCs. In conclusion, exercise training results in myocardial mass remodeling through both myocyte hypertrophy as well as hyperplasia. The latter is due to the activation and ensuing differentiation of CSCs into newly-formed myocytes, with increased IGF-1 expression playing a key role in this process.

Authors have confirmed where relevant, that experiments on animals and man were conducted in accordance with national and/or local ethical requirements.

C18

Phospholamban is required to increase sarcoplasmic reticulum calcium content during β-adrenergic stimulation

S.J. Briston, K.M. Dibb, A.W. Trafford and D.A. Eisner

Unit of Cardiac Physiology, University of Manchester, Manchester, UK

Sarcoplasmic reticulum (SR) Ca content is important in determining the size of the systolic Ca transient. The increase of systolic Ca transient amplitude produced by β-adrenergic stimulation results, at least in part, from an increase of SR Ca. One well-established mechanism for the increase of SR Ca is due to phosphorylation of phospholamban thus increasing SR Ca uptake by the SR Ca-ATPase (SERCA) (Tada et al, 1974). We have investigated whether other mechanisms can contribute to the increase of SR Ca.

Ventricular myocytes were isolated from wild-type (WT) (C57Bl/6J) and phospholamban knockout ($PLN^{-/-}$) mice killed by cervical dislocation. Whole cell patch clamp studies were performed at 37°C using a Cs^+ based pipette solution containing the Ca indicator Fluo-5F. Myocytes were voltage clamped and stimulated with depolarising steps to 10 mV from a holding potential of -60 mV. SR Ca content was measured by integrating the sodium-calcium exchange (NCX) current produced by rapid application of 10 mM caffeine. Data are presented as mean ± S.E.M with the Students t-test used for statistical analyses.

β-adrenergic stimulation (100 nM isoprenaline) increased the systolic Ca transient amplitude in WT and $PLN^{-/-}$ myocytes by 124±25% and 85±30% respectively. This was accompanied by an increase of the amplitude of the L-type Ca current from 11.8±0.8 to 14.9±1.0 pA/pF (n=12 myocytes) in WT and 9.1±0.9 to 12.9±1.2 pA/pF (n=14 myocytes) in $PLN^{-/-}$. SR Ca content increased in WT from 69±2 to 86±5 $\mu mol.l^{-1}$ ($p<0.01$, n=12 myocytes). In contrast, in $PLN^{-/-}$ myocytes, β-adrenergic stimulation decreased SR Ca content from 174±17 to 127 ±12 $\mu mol.l^{-1}$ ($p<0.01$, n=14 myocytes).

These results show that phosphorylation of phospholamban is required for the increase in SR Ca content in response to β-adrenergic stimulation. Previous work (Trafford et al, 2001) has shown that increasing the L-type Ca current (by increasing external Ca concentration) decreases SR Ca content. This result was attributed to the fact that although an increase of L-type Ca current increases Ca entry into the cell, it also triggers more Ca release from the SR and thence more Ca efflux from the cell tending to deplete the SR. A similar mechanism can account for the observed decrease of SR Ca content during β-adrenergic stimulation in the absence of phospholamban. We conclude that β-adrenergic stimulation results in a net increase in SR content due to the effects of phospholamban phosphorylation.

Tada *et al*. 1974. *J Biol Chem*. **249**:6174-80.

Trafford *et al*. 2001. *Circ Res*. **88**:195-201.

This work was supported by the British Heart Foundation.

Authors have confirmed where relevant, that experiments on animals and man were conducted in accordance with national and/or local ethical requirements.

C19

Beta adrenergic stimulation increases the sarcoplasmic reticulum threshold for arrhythmogenic diastolic calcium release in rat ventricular myocytes

T. Kashimura, A.W. Trafford, D.A. Eisner and L. Venetucci

Cardiovascular Research Group, Manchester University, Manchester, UK

In cardiac myocytes calcium release occurs by the process of calcium induced calcium release (CICR). The action potential activates the L-type Ca current and the resulting Ca influx triggers the opening of the sarcoplasmic reticulum (SR) Ca release channel (ryanodine receptor, RyR). However, if the amount of Ca stored in the SR reaches a critical or threshold concentration, waves of CICR can occur during diastole independent of the action potential (also known as diastolic Ca release). Beta adrenergic stimulation produces Ca waves. It has been suggested that this occurs by phosphorylation of the RyR that increases its activity and lowers the SR threshold for diastolic Ca release.(Marx et al., 2000). An alternative explanation, however, of the ability of beta adrenergic stimulation to produce

Ca waves is via an increase of SR Ca content secondary to phosphorylation of phospholamban and thence stimulation of the SR Ca-ATPase (SERCA).
The main objective of this study was to directly measure the effects of beta adrenergic stimulation on the threshold for diastolic Ca release. Experiments were performed in rat ventricular myocytes patch clamped using the perforated patch technique. Cells were held at -40 mV and stimulated at 0.5 Hz using voltage steps to 0 mV at room temperature. Diastolic Ca waves were induced by applying high external Ca (4mM) and long depolarizing steps (500 msec). 1 μM isoprenaline was applied to test the effects of beta adrenergic stimulation. When stimulation was stopped a few Ca waves were observed immediately after the last Ca transient. Caffeine (5 mM) and Butanedione Monoxime (10 mM) were applied immediately after the last Ca wave in both conditions to determine the threshold SR Ca content for diastolic Ca waves. The integral of the caffeine induced current was used to quantify SR Ca content. The threshold for spontaneous Ca release was significantly higher in the presence of isoprenaline (94±15 μmol/l in 4 Ca and 123±14 μmol/l in 4 Ca + isoprenaline; n=8, P=0.001, paired t test). On the basis of these data we conclude that beta adrenergic stimulation increases the SR threshold for spontaneous Ca release. This result is not what would be expected from phosphorylation of the RyR. It may be due to stimulation of SERCA making it more difficult for Ca waves to propagate (O'Neill et al., 2004).

Marx SO, Reiken S, Hisamatsu Y, Jayaraman T, Burkhoff D, Rosemblit N, & Marks AR (2000). Cell 101, 365-376.

O'Neill SC, Miller L, Hinch R, & Eisner DA (2004). . J Physiol (Lond) 559, 121-128.

British Heart Foundation

Authors have confirmed where relevant, that experiments on animals and man were conducted in accordance with national and/or local ethical requirements.

C20

Effects of atrial fibrillation on electrically heterogeneous human atria: a computer modelling study

S. Kharche[1], J. Stott[1], P. Law[1], H. Dobrzynski[2] and H. Zhang[1]

[1]School of Physics and Astronomy, University of Manchester, Manchester, UK and [2]School of Medicine, University of Manchester, Manchester, UK

Introduction: Human atria are composed of electrically heterogeneous tissues [1]. We postulated that electrical remodelling induced by chronic atrial fibrillation (AF) enhances heterogeneity and facilitates AF.
Methods: We modified the Courtemanche *et al.* [2] model to simulate action potentials (APs) in human atrial cells types, *i.e.* atrial chambers (CRN), pectinate muscle (PM), cristae terminalis (CT), atrioventricular ring (AV ring) and atrial appendage [1]. We further incorporated experimental data of *AF induced electrical remodelling* (AFER) based on studies by Bosch *et al.* (AF1) [3] and Workman *et al.* (AF2) [4]. Single cell models were then incorporated into spatial models with realistic 2D geometry of human atria. Using these models, we quantified the effects of AFER on atrial AP profiles, AP duration (APD_{90}), rate dependency of AP duration (APDr), effective refractory period (ERPr) and intra-atrial conduction velocity (CVr). Effects of AFER on atrial tissue's vulnerability to uni-directional conduction block (VW) and the dynamical behaviour of re-entrant excitation waves in 2D electrically heterogeneous realistic models were studied.
Results: AFER inhomogenously abbreviated atrial APD_{90}'s with the largest reduction in the CT (Control: 333.0 ms; AF1: 136.6 ms; AF2: 181.0 ms) and the smallest reduction in the AV ring APD (Control: 253.2 ms; AF1: 92.0 ms; AF2: 122.5 ms). The effects of AF on cellular APD_{90}'s are shown in Figure 1. AFER reduced ERP dramatically for all tissue types. AFER reduced atrial excitability leading to a slower intra-atrial electrical conduction. However, AFER facilitated electrical conduction at much higher pacing rates compared to Control tissue. The measured maximal rates for atrial excitation conduction in CT tissue were 198, 421, 325 and 198 beats/minute for the Control, AF1 and AF2 cases respectively. AFER reduced tissue's VW in all tissue types. AFER induced inhomogeneous alterations in the electrical properties had a direct impact on the dynamical behaviours of re-entrant waves. Under Control conditions re-entrant waves self terminated with a life span of 1800 ms. However, under AF conditions, re-entrant waves were sustained and led to persistent erratic propagating wavelets.
Conclusions: AFER augmented spatial heterogeneity in atrial electrical properties, which is pro-arrhythmic as it helped sustain re-entrant waves. This study provides an insight into the mechanisms underlying "AF begets AF".

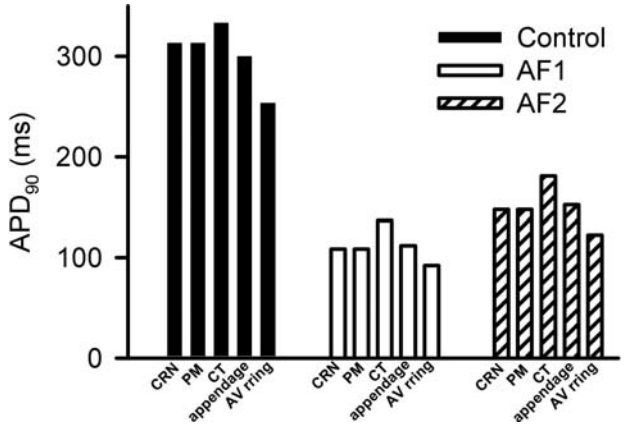

Figure 1. APD_{90} heterogeneity in human atrium and the effects of AF on APD_{90}. Data shows APD_{90} for atrial chambers (CRN), PM, CT, appendage and AV ring under Control (solid bars), AF1 (empty bars) and AF2 (striped bars) conditions. The average APD_{90} reductions were 65% due to AF1 and 52% due to AF2.

Seemann G. *et al.* (2006). *Phil. Trans. Roy. Soc. A.* **364(1843)**, 1465-1481.

Courtemanche M. *et al.* (1998). *Am. J. Physiol.* **275**, H301-H321.

Bosch RF *et al.* (1999). *Cardiovascular Res.* **44**, 121-131.

Workman AJ *et al.* (2001). *Cardiovascular Res.* **52**, 226-235.

This work was supported by the British Heart Foundation (Grant no. PG/06/140).

Authors have confirmed where relevant, that experiments on animals and man were conducted in accordance with national and/or local ethical requirements.

C21

Differences in intracellular calcium homeostasis between ovine atrial and ventricular myocytes

J.D. Clarke, K.M. Dibb and A.W. Trafford

Cardiac Physiology, University of Manchester, Manchester, UK

A number of biochemical and structural differences have been reported between atrial and ventricular tissue. Notably atrial myocytes have limited or no t-tubules, smaller volume and lower ratio of the sarcoplasmic reticulum calcium ATPase (SERCA) to its inhibitory peptide phospholamban. Since excitation contraction coupling in the ventricle is largely initiated in the t-tubule regions and that sarcoplasmic reticulum (SR) calcium content regulates systolic calcium this study aimed to characterise any alterations in intracellular calcium homeostasis between atrial and ventricular myocytes.

All experiments were performed on freshly isolated single cardiac myocytes obtained from the left ventricular midmyocardium or left atrium using an enzymatic method. Sheep were sacrificed humanely by the intravenous administration of pentobarbitone sodium (200mg/kg). Fluo-5F was used to measure intracellular calcium. All experiments were performed at 37ºC and used the perforated patch voltage clamp technique. SR calcium content was quantified by discharging the SR calcium store with caffeine (10mmol/L) and integrating the resulting sodium-calcium exchange current. Data are presented as mean ± SEM. Statistical significance was determined using a students t-tests.

Ventricular myocytes were 9% longer and 59% wider than atrial cells ($p<0.05$, n = 214-327). Peak L-type calcium current was smaller in atrial cells (3.3 ± 0.7 vs 2.3 ± 0.2 pA/pF n = 10-39, $p<0.05$). However, both the amplitude of the systolic calcium transient (F/F0, 0.8 ± 0.1 vs 1.5 ±0.1, $p<0.05$, n = 9-35 cells) and the rate of decay of the systolic transient (5.3 ± 0.4 vs 8.2 ± 0.3 s^{-1}, n = 8-36 <0.001) were increased in atrial cells. The SERCA mediated calcium removal rate was calculated by subtracting the rate of decay of the caffeine evoked calcium transient from that of the systolic calcium transient and was accelerated in atrial cells (4.2 ± 0.6 vs 7.4 ± 0.4 s^{-1}, n = 7-30, $p<0.001$). This latter observation is consistent with an increased SR calcium content in atrial cells (56.0 ± 6.8 vs 238.1 ± 17.8 μmol/l, n = 7-28, $p<0.0001$).

In summary there are substantial differences in intracellular calcium homeostasis between atrial and ventricular myocytes isolated from the sheep. We propose that previously reported alterations in the ratio of SERCA to phospholamban explains the faster SR dependent calcium uptake and SR calcium content in atrial cells. Additionally, the increased SR calcium content provides a possible mechanism for the larger systolic calcium transient in atrial cells despite the smaller L-type calcium current. It remains to be determined if these alterations are important in explaining the higher frequency of atrial arrhythmias observed in clinical practice.

Supported by The British Heart Foundation and European Union (STREP Project "NORMACOR," 6th European Framework Program)

Authors have confirmed where relevant, that experiments on animals and man were conducted in accordance with national and/or local ethical requirements.

C22

I_{K1} remodelling in the ageing heart

M. Richards, A.W. Trafford and K.M. Dibb

Unit of Cardiac Physiology, University of Manchester, Manchester, UK

Ageing is a major risk factor for the development of heart failure and arrhythmias. The inward rectifier potassium current, I_{K1}, is crucial for terminal phase repolarisation and stabilising the resting membrane potential of cardiac myocytes. Reductions in I_{K1} contribute to an increased susceptibility to arrhythmias in heart failure (Pogwizd *et al*. 2001). Previously, we have shown an increase of I_{K1} in left ventricular midmyocardial myocytes that may reduce susceptibility to arrythmias. We investigated the expression of I_{K1} across the left ventricular free wall of young and old sheep as well as the sensitivity of I_{K1} to β-adrenergic stimulation.

Young adult (18 months old) and old sheep (>8 years) were euthanased with 200 $mg.kg^{-1}$ intravenous pentobarbitone. Myocytes were isolated from the endo-, midmyo- and epicardial layers of the left ventricular free wall by collagenase digestion. I_{K1} currents were recorded using the whole-cell voltage clamp technique with a K^+-based pipette solution at 37ºC. Statistical analyses were carried out using 1-way ANOVA or a Mann-Whitney rank sum test for non-normally distributed populations.

Steady-state I_{K1} was uniform across the wall in young hearts, whereas the old hearts had developed a transmural I_{K1} gradient (endo > mid ≈ epi; $P < 0.05$). The I_{K1} gradient in the old hearts was due to a greater channel conductance and a rightward shift in Vmid in the endocardial myocytes ($P < 0.05$), with no difference in slope conductance (Vc). Steady-state I_{K1} in both endo- and midmyocardial myocytes was increased in the old sheep (young vs old, mid: -1.31 ± 0.10 vs -2.00 ± 0.18 pA/pF, n = 20 and 27; $P < 0.05$; endo: -1.55 ± 0.16 vs -5.09 ± 1.13 pA/pF, n = 10 and 11; $P < 0.05$). These changes were accompanied by an increased channel conductance and a rightward shift in Vmid, with a decrease in slope conductance (Vc). β-adrenergic stimulation using isoprenaline (100nM) reduced steady-state I_{K1} in old endocardial myocytes only (-5.09 ± 1.13 vs -2.22 ± 0.30 pA/pF, n = 11 and 8; $P < 0.05$). Channel conductance was decreased with isoprenaline with no change in Vmid, but an increase in slope conductance (Vc). β-adrenergic stimulation reduced steady-state I_{K1} to amplitudes similar to those in old epi- and midmyocardial myocytes and was sufficient to eliminate the steady-state I_{K1} transmural gradient present in the old hearts.

In conclusion, we show that I_{K1} is remodelled in aged ventricular myocytes. Increases in I_{K1} in the endo- and midmyocardial layers may be an important mechanism in stabilising the resting membrane potential and limiting the prolongation of the action potential duration associated with ageing (Dibb *et al*. 2004). β-adrenergic-induced inhibition of I_{K1} may increase the arrythmogenic potential in endocardial myocytes of old sheep

by preventing this mechanism thus increasing the dispersion of repolarisation in the old heart.

Pogwizd *et al*. (2001) *Circ Res* **88**: 1159.

Dibb *et al*. (2004) *J. Mol Cell Cardiol* **37**: 1171.

This work was supported by the British Heart Foundation.

Authors have confirmed where relevant, that experiments on animals and man were conducted in accordance with national and/or local ethical requirements.

C23

The plasticity of ion channel gene expression in the rat sinoatrial node

J. Tellez[1], H. Dobrzynski[1], J. Yanni[1], U. Mackiewicz[2], M. Maczewski[2], A. Beresewicz[2] and M.R. Boyett[1]

[1]Cardiovascular Medicine, University of Manchester, Manchester, UK and [2]Department of Clinical Physiology, Medical Center of Postgraduate Education, Warsaw, Poland

The sinoatrial (SA) node is the primary pacemaker of the heart. It is known that SA node dysfunction is associated with increasing age (Di Gennaro *et al*. 1987). In addition, a reduction in intrinsic sinus rate is associated with heart failure (Janse *et al*. 2004). Ion channels and their associated subunits are key to the pacemaker function of the SA node. We used quantitative PCR to investigate if there is an age-dependent change in ion channel gene expression in the SA node. We separately investigated if heart failure causes a change in ion change gene expression in the SA node.

For the study of ageing, 3 month (n=8) and 25 month (n=8) Wistar-Hanover rats were used. Heart failure was induced by generating an extensive myocardial infarction (caused by the ligation of the proximal left coronary artery performed under ketamine HCl and xylazine anaesthesia (100 mg/5 mg/kg body weight) injected intraperitoneally). Heart failure (n=8) and sham-operated (n=8) rats were used. In both studies, tissue was sampled from the right atrium and SA node (3 months post-operatively in the heart failure study). Ion channel gene expression was detected using quantitative PCR with an ABI 7900HT instrument with ABI Taqman probe assays. The study was conducted in accordance with Guide for the Care and Use of Laboratory Animals (US National Institutes of Health Publication No. 85-23, revised 1985).

82 gene transcripts were measured in the ageing study. Of these transcripts, with age 28% changed significantly in the atrial muscle and 23% changed in the SA node. In the SA node, these changes included significant increases in expression of transcripts responsible for $Na_v1.5$ (+33%) and $Ca_v1.2$ (+9%), which are responsible for the important inward currents, I_{Na} and $I_{Ca,L}$. With age, $K_v1.2$ (+61%) and $K_v4.2$ (+198%) transcript expression also increased in the SA node, whereas $K_v1.5$ (-40%) transcript expression decreased; these transcripts are responsible for important outward currents.

88 gene transcripts were measured in the heart failure study. Of these transcripts, with heart failure 7% changed significantly in the atrial muscle and 40% changed in the SA node. In the SA node, this included significant increases in expression of HCN4 (+63%), $Ca_v1.2$ (+55%) and $Ca_v3.1$ (+73%) transcripts, which are responsible for the important inward currents I_f, $I_{Ca,L}$ and $I_{Ca,T}$. In addition, the expression of $K_v1.2$ (+72%) and $K_v1.5$ (+85%) transcripts, which are responsible for important outward currents, increased in the SA node in response to heart failure.

These results show the dynamic nature of ion channel expression in the SA node. These results show that the expression of ion channels and their accessory subunits change in the SA node with age and during heart failure. These changes must contribute to the SA node dysfunction in the elderly and in heart failure.

Di Gennaro M et al. (1987) Basic Res Cardiol **82**, 530-536.

Janse MJ (2004) Cardiovasc Res **61**, 208-217.

This work was supported by the British Heart Foundation.

Authors have confirmed where relevant, that experiments on animals and man were conducted in accordance with national and/or local ethical requirements.

C24

0.1 mm cubic voxel reconstruction of transgenic hypertrophic mouse heart structure using diffusion tensor magnetic resonance imaging

A.P. Benson[1,4], S.H. Gilbert[1,4], O. Bernus[1,4], M.E. Ries[2], J.F. Ainscough[3,4], S.G. Ball[3,4] and A.V. Holden[1,4]

[1]Institute of Membrane and Systems Biology, University of Leeds, Leeds, UK, [2]School of Physics and Astronomy, University of Leeds, Leeds, UK, [3]Leeds Institute of Genetics, Health and Therapeutics, University of Leeds, Leeds, UK and [4]Multidisciplinary Cardiovascular Research Centre, University of Leeds, Leeds, UK

Transgenic mouse models in which human angiotensin II type 1 (AT1) receptors are expressed specifically in the heart have been developed (1). AT1 receptor expression can be temporally controlled both prior to and after birth to allow activation over discrete periods. The resultant controlled hypertrophy is apparent in whole hearts. Diffusion tensor magnetic resonance imaging (DT-MRI) was used to reconstruct, visualise and quantify the structure of these hearts. The primary eigenvector of the diffusion tensor provides a measure of fibre orientation, while the secondary and tertiary eigenvectors provide indices of sheet structure (2).

Fixed (4% formaldehyde/PBS; post mortem) and immobilised (in Fomblin) entire mouse hearts were imaged using a Bruker 9.4 T MR instrument and a standard reduced encoding diffusion-weighted gradient echo sequence at 20°C: 500 ms TR; 18.7 ms TE; diffusion gradients with 5 ms duration and 8.9 ms separation; b = 1130 s/mm^2. Voxel resolution was 0.1 mm^3. For each scan we acquired a single b0 image and diffusion-weighted images sensitised in each of 12 optimised directions (3). Single scan time for one heart was ~10 hours. We performed 6 scans per heart and calculated mean measurements at each voxel. Each heart model is a dataset of ~300 MB, and is available from us on request.

We have reconstructed, visualised and quantified the geometry and the fibre and sheet structure in these mouse hearts. These fibre and sheet directions can be mapped throughout the entire heart, and allow the application of fibre tracking algorithms. Thus, the combination of transgenic and DT-MRI methods enables the morphological changes in cardiac structure to be followed and quantified at different stages during the hypertrophic process.

These data add to a family of high-resolution digital models of cardiac geometry and architecture obtained from different species using DT-MRI (3,4), which can be used as platforms on which to run simulations of normal, pathological and pharmacologically-modified electrophysiology (5).

Sedo A *et al.* (2005). *Transgenic Res* **14**, 520.

Gilbert SH *et al.* (2007). *Eur J Cardiothorac Surg* **32**, 231-249.

Benson AP *et al.* (2008). *Proc Physiol Soc*, in press.

Dierckx H *et al.* (2008). *Heart Rhythm*, in press.

Benson AP *et al.* (2008). *Prog Biophys Mol Biol* **96**, 187-208.

Supported by the European Union through the BioSim Network of Excellence (LHSB-CT-2004-005137), the Medical Research Council, the British Heart Foundation, and the Multidisciplinary Cardiovascular Research Centre, University of Leeds.

Authors have confirmed where relevant, that experiments on animals and man were conducted in accordance with national and/or local ethical requirements.

C25

Maternal undernutrition affects the nutrient transport capacity of the mouse placenta

P.M. Coan, N. Daw, O.R. Vaughan, S.L. Finn and A.L. Fowden

Physiology, Development & Neuroscience, University of Cambridge, Cambridge, UK

Maternal diet during pregnancy is important in determining placental development. In farm animals, maternal undernutrition alters placental nutrient transfer but little is known about the effects of manipulating dietary composition on placental function in any species (1). This study examined transplacental transfer of nutrients transported by facilitated diffusion (14C-methyl-D-glucose) and active transport (14C-methyl aminoisobutyrate, MeAIB) in mice fed diets with varying protein content throughout pregnancy (term = 20 days, d). Group-housed pregnant mice were fed ad libitum either 23% (C23; n=66), 18% (C18; n=83), or 9% (C9; n=70) casein diets made isocalorific by carbohydrate supplementation. At 16d and 19d, mice were anaesthetised (10ul/g fentanyl-fluanisone:midazolam:water, 1:1:2, ip) before in vivo measurement of unidirectional materno-fetal flux of each tracer (2). After maternal cervical dislocation, placentas and fetuses were weighed. Fetuses were decapitated and dissolved in Biosol for scintillation counting. Transplacental tracer clearance was calculated as μl.min-1.g-1 placenta using maternal plasma and accumulated fetal radioactivity (3). All procedures for carried out under the Animal (Scientific Procedures) Act 1986. Results are means ± SE. Statistical significance was assessed by one way ANOVA.

MeAIB clearance in the C9 group matched the C23 group, both having significantly greater clearance than the C18 group at each age (Table 1). However, at E16, glucose clearance was greater in the C9 and C18 groups than the C23 group (Table 1). By E19, glucose clearance was greatest in the C9 group with both C18 and C23 groups transferring significantly less (Table 1).

The results show that maternal dietary composition alters placental nutrient transport capacity with differential effects on MeAIB and glucose transport in late gestation. Upregulation of placental glucose transfer in the mice fed the lowest protein diet may help meet fetal nutrient demands for growth. Variations in the relative proportions of nutrients supplied to the fetus due to dietary-induced adaptations in placental nutrient transport may programme tissue development in utero with consequences long after birth (1).

Transplacental MeAIB and glucose clearance with respect to maternal dietary protein content at days 16 and 19 of mouse pregnancy (n= > 9 litters per group).

	MeAIB		Glucose	
Isocalorific diets	16d	19d	16d	19d
23% casein diet	50±4 a	147±14 a	68±10 a	273±41 a
18% casein diet	31±3 b	108±9 b	148±18 b	244±49 a
9% casein diet	55±4 a	131±11 a,b	123±19 b	362±49 b

Values within columns with different letters (a,b) are significantly different from each other P<0.05

Fowden AL et al. (2008)J Neuroendocrinology 20, 439-450

Constancia M et al. (2005) Proc Natl Acad Sci USA 102, 19219-19224

Sibley CP et al. (2004) Proc Natl Acad Sci USA 101, 8204-8208

This study was funded by the BBSRC

Authors have confirmed where relevant, that experiments on animals and man were conducted in accordance with national and/or local ethical requirements.

C26

Gene expression changes observed in the placenta from different maternal diets provide evidence for possible candidates for gatekeeper genes in development

A. Richmond[1], L. Gambling[1], C. Mayer[2], S.C. Langley-Evans[3], S. McMullen[3], P. Taylor[4] and H.J. McArdle[1]

[1]The Rowett Research Institute, Aberdeen, UK, [2]Biostatistics Scotland, The Rowett Research Institute, Aberdeen, UK, [3]University of Nottingham, Loughborough, UK and [4]King's College London, London, UK

During pregnancy, the quality of diet a mother consumes is critical for the development of her fetus and a suboptimal diet can have deleterious consequences for the offspring, both short and long term. Studies have shown that a low protein, high fat or a low iron diet results in offspring that develop hypertension and obesity. This has lead to the Gatekeeper hypothesis, which suggests that diverse nutritional stresses affect common

actinomycin D and 10μM 4-amino-5-(4-chlorophenyl)-7-(t-butyl)pyrazolo[3,4,d]pyrimidine (PP2). Thus, 630ρgml^{-1} of androstanolone led to a 29.6±3% (n=8 fibre bundles) increase in P_o in the fast-twitch fibres and to a 21.1±3% (n=7) decrease in P_o in the slow-twitch fibres. From these results we suggest that androstanolone acts via the androgen receptor to increase the translation of a protein(s) that increases force production in fast-twitch skeletal muscle fibres but inhibits it in slow-twitch fibres.

Kuhn C (2002). Anabolic steroids. Rec Prog Horm Res 57, 411-434

This research was funded by the University of East Anglia and the J&P Salter Trust

Authors have confirmed where relevant, that experiments on animals and man were conducted in accordance with national and/or local ethical requirements.

C57

The influence of ageing on intracellular calcium homeostasis in sheep atrial myocytes

J.D. Clarke, A.W. Trafford, D.A. Eisner and K.M. Dibb

Unit of Cardiac Physiology, University of Manchester, Manchester, UK

Atrial fibrillation (AF) is the most common cardiac arrhythmia and is an important risk factor for stroke[1]. The risk of AF development is strongly age dependent and thus the prevalence of AF is increasing as society ages. Despite this little is known regarding how intracellular Ca handling in the atria is altered by the ageing process and if age associated remodelling predisposes the aged heart to arrhythmias. We have investigated if the sources and sinks of Ca in atrial myocytes are altered during the ageing process.

Young adult (18 months old) and old sheep (>8 years) were euthanased with 200 mg/kg^{-1} intravenous pentobarbitone. Myocytes were isolated from the left atrium by enzymatic digestion. Atrial myocytes were stimulated at 0.5Hz under voltage clamp control using the perforated patch clamp technique. Changes in $[Ca]_i$ were measured using Fluo-5F AM. All experiments were performed at 37ºC. Data are presented as mean ± SEM from n experiments and statistical analysis was carried out using a t-test.

Ageing resulted in atrial myocyte hypertrophy as measured by capacitance (60.5±2.2 and 72.8±2.8pF, young versus old; n=76 to 81 p<0.001). This was primarily due to a 20% increase in myocyte width in the aged heart (15.0±0.2 to 18.1±0.5μM; n=230 to 347 p<0.001) although a modest increase in cell length was evident. The amplitude of the systolic Ca transient was decreased in the aged atria (1.5±0.1 to 1.2±0.1 expressed as F/F0, young versus aged; n=35-38 p<0.05) and was associated with a decrease in peak L-type Ca current (2.3±0.2 to 1.8±0.1pA.pF^{-1}; n=39-47 p<0.05). The rate of decay of the systolic Ca transient was slowed in the aged atria and this was due to a decrease in SERCA function. Ca removal by sarcolemmal pathways was unaltered by ageing. Whilst a decrease in SERCA function and a decrease in systolic Ca transient amplitude both point to a reduction in SR Ca content, integration of the caffeine evoked Na-Ca exchanger current showed that SR Ca content was *increased* in the aged atria (p<0.01).

In summary, a decrease in the trigger for Ca induced Ca release (L-type Ca current) may underlie the reduction in Ca transient amplitude in the aged atria. It remains to be determined if this reduction is sufficient to fully account for the reduced Ca transient amplitude in the aged atria in the presence of increased SR Ca content. The mechanism and role of the age associated increase in SR Ca content remains unexplained and further work is required to determine if these changes are related to spatial characteristics of Ca release.

1) Carrol K, Majeed A. Trends in mortality and hospital admissions associated with atrial fibrillation in England and Wales. *Health Stat Quart* 2001;**9**:37–44.

This work was supported by the British Heart Foundation (JDC) and University of Manchester Stepping Stone Awards (KMD).

Authors have confirmed where relevant, that experiments on animals and man were conducted in accordance with national and/or local ethical requirements.

C58

Bone marrow-derived stromal cells home to and remain in the infarcted rat heart, but fail to improve function: an *in vivo* MRI study

D.J. Stuckey[1], C.A. Carr[1], L. Tatton[2], D.J. Tyler[1], S.J. Hale[2], D. Sweeney[2], J.E. Schniedar[1], E. Martin-Rendon[2], G.K. Radda[1], S.E. Harding[3], S.M. Watt[2] and K. Clarke[1]

[1]Department of Physiology, Anatomy and Genetics, University of Oxford, Oxford, UK, [2]National Blood Service, Oxford, UK and [3]Imperial College, London, UK

Basic and clinical studies have shown that bone marrow cell therapy can improve cardiac function following infarction (1). In experimental animals, reported stem cell-mediated changes range from no measurable improvement to the complete restoration of function (2), whereas in the clinic the average improvement in left ventricular ejection fraction is 2-3% (3). A possible explanation for the discrepancy between basic and clinical results is that few basic studies have used the MRI methods that were used in clinical trials for measuring cardiac function. Consequently, we employed cine MRI to determine the effect of bone marrow stromal cells (BMSCs) on cardiac function in rats. Wistar rat BMSCs were isolated from tibias and femurs, cultured for 21 days, characterized using flow cytometry and labeled with iron oxide particles and a fluorescent marker to allow in vivo cell tracking and ex vivo cell identification, respectively (4). Neither label affected in vitro cell proliferation or differentiation. Wistar rats were anaesthetised with 2.5% isoflurane in O2 and the coronary artery was occluded. BMSCs or control media were either injected into the infarct periphery 10 minutes after infarction (n = 34) or infused systemically 1 or 3 days after infarction (n = 30). MRI was used to measure cardiac morphology and function and to determine cell distribution for 10 weeks after infarction and cell therapy. In vivo MRI, histology and cell re-isolation confirmed successful BMSC delivery and retention within the myocardium throughout the experiment (Figure). However, no significant improvement in any measure of cardiac morphology or function was observed at any time (Table). We conclude that cultured BMSCs are not the optimal cell population to treat the infarcted heart.

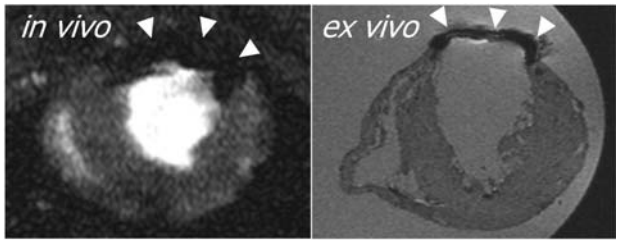

In vivo and ex vivo MR images of an infarcted rat heart. Arrows indicate position of BMSC engraftment

			BMSC treated groups		
	Sham	Control	i.m. @ 10 min	i.v. @ 1 day	i.v. @ 3 days
	(6)	(18)	(24)	(18)	(4)
Ejection fraction (%)					
1 week	82 ± 1	53 ± 2	54 ± 3	54 ± 2	54 ± 7
4 weeks	80 ± 2	54 ± 2	58 ± 3	54 ± 2	56 ± 8
10 week	82 ± 1	55 ± 2	54 ± 4	-	-
Scar size (% LV wall)					
1 week	0	20 ± 3	18 ± 2	20 ± 2	14 ± 7
4 weeks	0	19 ± 3	16 ± 2	19 ± 2	15 ± 7
10 week	0	16 ± 3	16 ± 3	-	-

Ejection fractions and scar sizes measured using in vivo MRI up to 10 weeks after myocardial infarction and BMSC administration. Mean ± sem.

Wollert KC & Drexler H. (2006) Curr Opin Cardiol 21, 234.

Laflamme MA & Murry CE. (2005) Nat Biotechnol 23, 845.

Saha M, et al. (2006) Heart 92, 1717.

Stuckey DJ, et al. (2006) Stem Cells 24, 1968.

This work was supported by the British Heart Foundation.

Authors have confirmed where relevant, that experiments on animals and man were conducted in accordance with national and/or local ethical requirements.

C59

Clustering of protein kinase A-dependent Cl^- channels in guinea-pig cardiac myocytes

A.F. James[1,2], Y. Okada[2] and R. Sabirov[2]

[1]Department of Physiology & Pharmacology, University of Bristol, Bristol, UK and [2]Department of Cell Physiology, National Institutes for Physiological Sciences, Okazaki, Japan

A number of Cl^- currents have been identified in cardiac myocytes and these may contribute both depolarising inward current and repolarising outward current. Of these, a current activated by the cAMP/protein kinase A (PKA) pathway has been suggested to play a role in action potential repolarisation in the presence of β-adrenoceptor agonism. A cardiac isoform of the cystic fibrosis transmembrane conductance regulator, cftr, has been suggested to contribute to this current. Considerable heterogeneity in the functional expression of certain ion channels has been shown between the t-tubule membrane and the surface sarcolemma. However, there is very little information regarding the localization of PKA-dependent Cl^- channels in cardiac myocytes. We have attempted to address this question using a combination of scanning ion conductance microscopy and cell-attached recording (Gu *et al.,* 2005), from isolated guinea-pig ventricular myocytes. Guinea-pig cardiomyocytes were isolated by mechanical disruption following retrograde perfusion of the aorta with a collagenase-containing Tyrode's solution. Pipettes (typically 15–30 MΩ) were filled with a recording solution in which permeant cations had been replaced with N-methyl-D-glutamate and cells superfused with a normal Tyrode's solution at room temperature. Using the pipette current as a feedback signal, 10μmx10μm scans of the cell surface were conducted. Data are presented as mean ± SEM. Grooves in the cell surface with a spacing of 2.0±0.1μm (*n*=30) could be identified, which were assumed to correspond to the z-line grooves. The pipette was then directed to a location on the cell surface identified in the image and, after formation of the giga-seal, on-cell recordings were made. Cells were superfused with an activating cocktail of 5μM isoprenaline/10μM forskolin/50μM isobutyl methylxanthine (IBMX), which activated anion-selective currents in 6/38 recordings. Membrane potentials within the patch were calculated as the difference between the resting membrane potential (RMP) and the pipette potential, assuming RMP = -80mV. Currents were typically large and noisy, making it difficult to distinguish unitary channel currents. The mean pipette current ranged from 90.8±14.3pA at +100mV to -27.1±3.6pA at -80mV and reversed at -32.3±2.6mV (*n*=6). Current activity was lost on excision of the patch and, in 2 patches where this was attempted, could be recovered by application of PKA catalytic subunit to the cytosolic surface. While the majority of current were recorded from the 'scallop' between z-grooves, current activity was also recorded within the z-grooves. These data are consistent with the suggestion that PKA-activated Cl^- channels occur in clusters containing >100 channels within the sarcolemma of guinea-pig ventricular myocytes.

Gu Y, Gorelik J, Spohr HA, Shevchuk A, Lab MJ, Harding SE, Vodyanov I, Klenerman D & Korchev YE. (2002). High-resolution scanning patch-clamp: new insights into cell function. FASEB J 16, 748-750.

Authors have confirmed where relevant, that experiments on animals and man were conducted in accordance with national and/or local ethical requirements.

C60

FTY720 attenuates ischemia-reperfusion damage in the rat's atrio-ventrivular node preparations

E. Eroume A Egom[1], H. Musa[1], K. Yunbo[2], J. Solaro[2] and M. Lei[1]

[1]Division of Cardiovascular and Endocrine Sciences, University of Manchester, Manchester, UK and [2]Department of Physiology and Biophysics and center for cardiovascular research, University of Illinois, Chicago, IL, USA

Organ dysfunction followed by single-organ, or even multi-organ failure, due to ischaemia-reperfusion injury (I/RI) is a common complication in transplant, liver, trauma, and heart surgery (Clavien et al.). Here we report that FTY720, an analogue

of sphingosine 1-phosphate, attenuates ischemia-reperfusion damage in the rat's atrio-ventricular node (AVN) preparations. Isolated rat AVN was prepared according to established method (Lei, Jones et al. 2004) and fixed in a tissue-perfusion chamber. The Preparation was superfused with control oxygenated Tyrode solution at a rate of 4 ml/min at 37 0C through a heat exchanger, then exposed to ischemic-like condition (omission of glucose and adjusted pH to 6.6 based on Tyrode solution) for 15 mins, the preparation was finally re-perfused with control Tyrode solution. Extracellular potentials were recorded by two bipolar electrodes from the preparation. The cycle length (CL) of the AVN preparations without treatment of FTY720 was prolonged by 67 % and 17 % in ischemia (CL: 716 ± 21 ms, n= 7) and reperfusion (501 ± 21 ms, n=7) conditions from the control condition (CL: 429 ± 18 ms, n = 7). The CL of AVNs treated with 25 nM FTY720 for 15 mins was prolonged by 5% and 15% in ischemia condition (CL: 446 ± 71 ms, n= 8) and reperfusion conditions (494 ± 70 ms, n=8) from the control condition (CL: 428±10 ms, n=8), the prolongation of CL is therefore significantly less than these preparations without FTY720 treatment.

Our results indicate that FTY720 significantly attenuates ischemia-reperfusion damage in the rat's AVN preparations and it represents a new approach to treatment of the many clinical disorders in which ischemia-reperfusion occurs. The mechanism for FTY720 protective effect requires a further investigation.

Clavien, P. A., et al. "Lymphocyte adherence in the reperfused rat liver: mechanisms and effects." Hepatology 17.1 (1993): 131-42.

Lei, M., S. A. Jones, et al. (2004). "Requirement of neuronal- and cardiac-type sodium channels for murine sinoatrial node pacemaking." J Physiol (Lond) 559(3): 835-848.

The work was supported by the Wellcome Trust (ML).

Authors have confirmed where relevant, that experiments on animals and man were conducted in accordance with national and/or local ethical requirements.

C61

Effects of hydrogen peroxide on calcium handling in rat ventricular myocytes

D.J. Greensmith, M. Nirmalan and D.A. Eisner

School of Medicine, University of Manchester, Manchester, Greater Manchester, UK

Hydrogen peroxide (H_2O_2) can be used to mimic intra and extracellular reactive oxygen species generation in disease states such as sepsis. Goldhaber *et al*. (1994) studied the effects of H_2O_2 on calcium handling in the ventricular myocyte at room temperature. As the cytoxicity of H_2O_2 is temperature dependent, it is important to understand its effect at physiological temperatures.

Male Wistar Rats were humanely killed by cervical dislocation in accordance with The Home Office Schedule 1 regulations. Ventricular myocytes were isolated via enzyme digestion and loaded with Fluo-3AM for cytoplasmic calcium ($[Ca^{2+}]_i$) measurement. Membrane currents were measured via perforated patch under voltage clamp conditions. Cell length was measured via video edge detection. Statistical significance was determined via the students t-test, and a value of less than 0.05 was deemed significant. Data is shown as mean±S.E.M.

200 μM H_2O_2 resulted in a progressive reduction in $[Ca^{2+}]_i$ transient amplitude (n=10, Control:272±29, H_2O_2:153±17 nmol/l, $p<0.0001$) and an increase in diastolic $[Ca^{2+}]_i$ (n=10, Control:93±5, H_2O_2:121±7 nmol/l, $p<0.0001$). Associated with this was a decrease in systolic cell shortening (n=7, Control:2.24±0.43, H_2O_2:0.87±0.14%, $p<0.05$), a reduced diastolic cell length (n=7, Control:123±8, H_2O_2:120±8 μm, $p<0.005$) and an increased relaxation time (n=7, Control:526±57, H_2O_2:746±118 ms, $p<0.05$) consistent with a reduced rate constant of $[Ca^{2+}]_i$ decay (n=10, Control:4.63±0.49, H_2O_2:3.79±0.36 s^{-1}, $p<0.005$). No change in the peak L-type calcium current was observed. L-type calcium influx was increased (n=10, Control:3.16±0.14, H_2O_2:3.43±0.18 μmol/l), whilst calcium efflux via the sodium calcium exchanger (NCX) was decreased (n=6, Control:1.26±0.13, H_2O_2:1.12±0.10 s^{-1}, $p<0.05$). Sarcoplasmic reticulum (SR) content was reduced (n=6, Control:95±11, H_2O_2:69±7 μmol/l, $p<0.05$), however the diastolic $[Ca^{2+}]_i$ rise still occurred with inhibition of SR function. Hyperpolarisation of the membrane voltage to -120 mV reversed the H_2O_2 induced $[Ca^{2+}]_i$ rise (n=9, -40 mV:2.57±0.98, -120 mV:-1.35±0.55 nmol/l s^{-1}, $p<0.05$). Reversal of $[Ca^{2+}]_i$ rise upon hyperpolarisation is consistent with the findings of Song *et al* (2006) who found H_2O_2 induced an increase in intracellular Na^+ ($[Na^+]_i$). Increased $[Na^+]_i$ could lead to increased $[Ca^{2+}]_i$ via reverse mode NCX activity.

These data suggest that H_2O_2 induced SR dysfunction reduces the $[Ca^{2+}]_i$ transient amplitude and is independent of L-type calcium current. H_2O_2 induced diastolic $[Ca^{2+}]_i$ rise occurs independently of the SR. This diastolic $[Ca^{2+}]_i$ rise may be due to increased $[Na^+]_i$ however increased Ca^{2+} influx combined with a impairment of Ca^{2+} removal mechanisms could be a contributing factor to H_2O_2 induced diastolic dysfunction.

Goldhaber JI *et al*. (1994). *Journal of Physiology* **477**, 135-147.

Song Y *et al*. (2006). *Journal of Pharmacology and Experimental Therapeutics* **318**, 214-222.

This work was supported by the British Heart Foundation and the University of Manchester Strategic Studentship Initiative.

Authors have confirmed where relevant, that experiments on animals and man were conducted in accordance with national and/or local ethical requirements.

C62

Antioxidant treatment ameliorates the deleterious effects of glucocorticoids on survival, somatic growth and cardiovascular development in the rat neonate

A. Adler, E.J. Camm, J.A. Hansell, H.G. Richter and D.A. Giussani

Physiology, University of Cambridge, Cambridge, UK

Glucocorticoids (GC) reduce chronic lung disease (CLD) in premature infants. However, studies have raised concern because

of adverse effects of GC on somatic growth and organ development[1]. Treatment of neonatal rats with dexamethasone (Dex) promotes adverse effects on heart structure and function in adulthood[2]. In humans, GC excess increases superoxide production and vascular dysfunction, effects that are resolved by vitamin C[3]. The aims of this study were to determine in rats: 1) the effects of neonatal Dex administration on early somatic growth and heart development, and 2) whether co-administration with vitamins C and E ameliorates any detrimental effects of GC.

Male Wistar pups received i.p. injections of Dexamethasone-21-phosphate (Dex; n = 7; 0.5, 0.3, 0.1 $\mu g.g^{-1}$) or Dex with vitamins C and E (DCE; n = 12; 200 $mg.kg^{-1}$ and 100 $mg.kg^{-1}$, respectively) on postnatal days 1-3 (P1-3); vitamins were continued from P4-6. Controls received equal volumes (10 $ml.kg^{-1}$) of saline (ctrl; n = 11) from P1-6. The tapering course of Dex used was adopted from a human clinical regimen used in preterm infants[4]. The doses of vitamins were adopted from studies in rats which showed successful antioxidant effects[5]. On P21, following euthanasia (0.2 mL, i.p., xylazine and ketamine), biometry measurements were taken and hearts were snap frozen for protein analysis. Antibodies against eNOS, Hsp90, and 4-hydroxynonenal (4-HNE) were used to assess oxidant stress. Data were analyzed by One-Way ANOVA + Tukey and chi-square test.

Compared to controls, Dex treatment reduced survival (ctrl: 96%; Dex: 70%, $P<0.05$), and promoted postnatal asymmetric growth restriction (body weight (BW) at P21 ctrl: 65.1 ± 2.7 *vs.* Dex: 50.9 ± 1.1 g, Ponderal index (PI) at P21 ctrl: 6.3 ± 0.1 *vs.* Dex: 7.4 ± 0.2 $kg.m^{-3}$, $P<0.05$). Western blot analysis revealed that, compared to controls, Dex increased 4-HNE (13%) whilst decreasing Hsp90 (-42%) and eNOS (-54%) expression ($P<0.05$). Addition of vitamins to Dex pups increased survival (DCE: 93%) and restored PI to control levels (6.7 ± 0.1 $kg.m^{-3}$, $P<0.05$), but did not alter the reduction in BW. In DCE pups, eNOS protein was restored to control levels and Hsp90 was reduced to a lesser extent (-22%), while 4-HNE remained upregulated (22%). In conclusion, Dex treatment of neonatal rats has detrimental effects on somatic growth and survival and promotes a decrease in proteins that may lead to increased oxidant stress and decreased NO bioavailability in the neonatal heart. Addition of antioxidant vitamins to Dex-treated pups ameliorates these effects. This study raises the possibility that combined treatment of premature infants with GC and antioxidants may be better than administration of GC alone in the treatment of CLD.

Liggins GC & Howie RN (1972). *Pediatrics* **50**, 515-525.

Iuchi T, Akaike M, Mitsui T, Ohshima Y, Shintani Y, Azuma H & Matsumoto T (2003). *Circ Res* **92**, 81-87.

de Vries WB, van der Leij FR, Bakker JM, Kamphuis PJ, van Oosterhout MF, Schipper ME, Smid GB, Bartelds B & van Bel F (2002). *Pediatr Res* **52**, 900-906.

Werner JC, Sicard RE, Hansen TW, Solomon E, Cowett RM & Oh W (1992). *J Pediatr* **121**, 500-501.

Oncu M, Gultekin F, Karaöz E, Altuntas I & Delibas N (2002). *Hum Exp Toxicol* **21**, 223-230.

Work supported by the Gates Cambridge Trust and the British Heart Foundation.

Authors have confirmed where relevant, that experiments on animals and man were conducted in accordance with national and/or local ethical requirements.

C63

Macro-molecular structure and function of cardiac titin

H.K. Graham[1], M.J. Sherratt[2] and A.W. Trafford[1]

[1]Cardiovascular Medicine, University of Manchester, Manchester, UK and [2]Tissue Injury and Repair, University of Manchester, Manchester, UK

Left ventricular diastolic dysfunction is characterised by slow and delayed ventricular relaxation, increased chamber stiffness and is associated with significant morbidity and mortality. Over the physiological sarcomere length range the passive stiffness of cardiac muscle is predominantly mediated by the giant muscle protein titin. This study aimed to characterise the macromolecular structure and nano-mechanical properties of titin populations by direct measurement of their axial mass and tensile strength.

Titin was extracted and purified from ferret left ventricular tissue, air dried on carbon support films and unstained specimens were visualised by scanning transmission electron microscopy (STEM). By using the tobacco mosaic virus (TMV) as a standard of mass per unit length (MUL), precise measurements of MUL were made at regular intervals along native titin molecules to generate an axial mass distribution (AMD). Titin nano-mechanical properties were quantified by molecular combing[1] of partially adsorbed molecules on a poly-l-lysine modified mica surface. The surface tension force induced by the progression of the receding meniscus during air drying applies a tensile force of ~160pN to the adsorbed molecules. Combed and uncombed molecules were visualised by atomic force microscopy (AFM). Titin appeared as relatively straight filaments of variable diameter when adsorbed to hydrophobic carbon films and visualised by STEM. The axial mass distribution of these filaments fitted a biomodal Gaussian which peaked at 6.5 kDa/nm and 15 kDa/nm (n=280).

Uncombed titin molecules, visualised by atomic force microscopy (AFM), appeared highly coiled. In contrast, combed molecules were straightened and aligned. Uncombed titin monomers ranged in length from 0.6 to 1.4 μm (n=40). Following molecular combing, Gaussian analysis revealed that monomer length increased from 1.2 to 1.7μm (n=42). Mean axial height was reduced following combing (0.62 ± 0.21 nm *vs* 0.58 ± 0.22 nm n=4000 $p<0.01$).

These observations are in agreement with previous theoretical predictions of the mass density of titin monomers and hence dimers[2]. The novel combination of STEM, molecular combing and AFM is capable of quantifying changes in titin structure and mechanical function induced by ageing and/or disease.

Sherratt MJ, Baldock C, Haston JL et al. *J Mol Biol* 2003 September 5;**332**(1):183-93.

Wang K, Ramirez-Mitchell R, Palter D (1984). *Proc Natl Acad Sci U S A* **81**(12), 3685-9.

The authors acknowledge the support of the British Heart Foundation. MJS is a Research into Ageing Senior Research Fellow.

Authors have confirmed where relevant, that experiments on animals and man were conducted in accordance with national and/or local ethical requirements.

C64

Effects of heat stress on left ventricular rotation and rotation rate in resting humans

E. Stöhr[1], J. González-Alonso[1], J. Pearson[1], L. Ali[2], H. Barker[2] and R. Shave[1]

[1]Centre for Sports Medicine and Human Performance, Brunel University West London, Uxbridge, Middlesex, UK and [2]Department of Anaesthetics, Ealing Hospital NHS Trust, Southall, Middlesex, UK

Introduction: Counter rotation in the left ventricular (LV) base and apex during systole and diastole plays an important role in the filling and emptying of the LV. Heat stress leads to increased cardiac work, evidenced by a rise in heart rate (HR) and cardiac output at rest. Whilst the influence of heat stress on LV dimensions has been assessed (Crandall *et al*. 2008) the effects on cardiac twisting (systolic rotation) and untwisting (diastolic rotation) remain unknown. In order to further elaborate the influence of passive heating on LV function, the present study sought to evaluate the hypothesis that passive heat stress increases LV rotation and rotation rate. Methods: Six active male subjects (21±2yr) completed the study, remaining fully hydrated throughout. Measurements were made at 4 different thermal conditions: 1) Control (Tcore ~37°C, Tskin ~32°C), 2) skin hyperthermia (Tc ~37°C, Tsk ~36°C), 3) skin and mild core hyperthermia (Tc ~38°C, Tsk ~37°C), and 4) high skin and core hyperthermia (Tc ~39°C, Tsk ~38°C). Echocardiographic images were acquired at each stage of heat stress. Two-dimensional images were analysed for LV basal and apical peak rotation (ROT_{bas}, ROT_{api}) and rotation rates ($ROTR_{bas}$, $ROTR_{api}$) and ejection fraction (EF). Mean arterial pressure (MAP) was measured online via a canula inserted in the radial artery. HR was assessed throughout the trial using a three lead ECG. A repeated measures ANOVA was used to detect effects over time and paired student t-test was applied post-hoc to ascertain differences between conditions. Alpha was set at 0.05, Bonferroni adjustment was made for repeated comparisons. Results: ROT_{bas} increased significantly between skin hyperthermia and high skin and core hyperthermia (-6.5±3.1 vs. -11.3±3.5°, $p<0.05$). ROT_{api} ($p>0.05$) was unaltered. Systolic and late diastolic $ROTR_{bas}$ increased significantly between control and high skin and core hyperthermia (-88±13 vs. -161±48 s^{-1} & 25±10 vs. 76±19 s^{-1}, $p<0.05$). Late diastolic $ROTR_{api}$ increased significantly between control and high skin and core hyperthermia (-6±12 vs. -47±31 s^{-1}, $p<0.05$). EF also increased between control and high core hyperthermia (61±4 vs. 76±7%, $p<0.05$). MAP remained constant throughout the experiment ($p>0.05$) and HR significantly increased between control and high core hyperthermia (62±14 vs. 119±14 beats*min^{-1}, $p<0.05$). Conclusion: Similar to previous studies we demonstrated an increase in systolic function with passive heating, as evidenced by an increase in EF. Our findings suggest that heat stress also increases LV systolic ROT_{bas}, systolic and late diastolic $ROTR_{bas}$ and late diastolic $ROTR_{api}$. The enhanced twisting and untwisting rate of the LV may facilitate the pronounced increase in EF observed with increased core temperature.

Crandall CG *et al*. (2008). *J Physiol* **586**, 293-301.

Supported by the Gatorade Sports Science Institute.

Authors have confirmed where relevant, that experiments on animals and man were conducted in accordance with national and/or local ethical requirements.

C65

Distinct structure and pharmacological properties of the precapillary sphincters in ureteric microvasculature. *In situ* imaging study

L. Borisova[1], D. Eisner[2], S. Wray[1] and T. Burdyga[1]

[1]The Physiological Laboratory, University of Liverpool, Liverpool, UK and [2]Unit of Cardiac Physiology, University of Manchester, Manchester, UK

It has long been recognized that the control of intermittent blood flow in capillaries is controlled by the "precapillary sphincters". However, until now it has not been clear what type of cells performs this important physiological function. Suggestions are: smooth muscle cells (SMC) originating from precapillary arterioles (PA) (Rhodin 1967) encircling capillary orifices, precapillary pericytes expressing contractile proteins (Hirshi et al, 1996, Sims 1986) and even specialised contractile endothelial cells (Ragan et al, 1988). However, to the best of our knowledge no study has investigated the properties of these cells *in situ*. In the present study we used high-resolution X-Y-Z and fast temporal confocal imaging of *in situ* ureteric microvessels loaded with the Ca^{2+}-sensitive indicator Fluo-4 (Burdyga et al, 2003) in order to investigate morphology, Ca^{2+} signalling and mechanical activity of SMC and precapillary pericytes comprising rat ureteric precapillary sphincter (PS) (inner diameter, i.d.<10μm). The effects of central (phenylephrine, PhE) and local (endohelin-1, ET-1) factors as well as caffeine - a powerful vasoconstrictor on PA (i.d.=15-25μm) and PS (i.d.<10μm) have been investigated.

We have defined two types of PS: type 1 (length >40μm) in which endothelium was encircled by both SMC and precapillary pericytes; and type 2 (length <40μm) in which endothelium was encircled by a group of precapillary pericytes only. SMC made three full turns around the endothelium and occupied a length of 9.81±0.21μm (n=12). Precapillary pericytes formed an asymmetrical coat with thick massive body located on one side of the vessel giving several finger like processes wrapping around endothelium. Each precapillary pericyte occupied a length of 10.10±0.48μm (n=15).

SMC of PA responded with Ca^{2+} oscillations and vasomotion when stimulated by either PhE (10μM) or ET-1 (10nM). Also in these myocytes, caffeine at low concentrations (0.5-1mM) enhanced or initiated Ca^{2+} sparks and at higher concentrations (2-5mM) produced Ca^{2+} waves and vasoconstriction. In marked contrast, SMC of PS were immune to caffeine (1-10mM) and PhE (10-100μM) but readily responded to ET-1 with Ca^{2+} oscillations and vasoconstriction. Precapillary pericytes were also

Kamkin A et al. (2005). Electrical interaction of mechanosensitive fibroblasts and myocytes in the heart. *Basic Res Cardiol*. **V100**, 337-345.

Martinac B & Kloda A. (2003). Evolutionary origins of mechanosensitive ion channels. *Prog Biophys Mol Biol*. **82**, 11-24.

White E. (2006). Mechanosensitive channels: Therapeutic targets in the myocardium? *Curr Pharm Des*. **12**, 3645-3663.

We would like to acknowledge the help we have received from Mike Greenwood.

Authors have confirmed where relevant, that experiments on animals and man were conducted in accordance with national and/or local ethical requirements.

PC16

The role of reverse-mode NCX in the contractility of the rainbow trout heart

H. Shiels, A. Allen, A. Smith, J. Hall and R. Birkedal

Faculty of Life Sciences, University of Manchester, Manchester, UK

The Ca2+ that initiates contraction in the rainbow trout heart arrives at the myofilaments primarily through L-type Ca2+ channels in the sarcolemmal membrane (Vornanen et al., 2000). However, at specific times during the action potential, Ca2+ can also be brought across the sarcolemma by the Na+-Ca2+ exchanger (NCX) operating in reverse-mode (revNCX)(Hove-Madsen et al., 2000). The relative importance of this route of Ca2+ influx was assessed in single isolated cardiac myocytes and isolated muscle preparations using the specific inhibitor of revNCX, KB-R7943.

Rainbow trout (range 75 g to 600 g body weight) were killed humanely (UK Home Office Schedule 1 method). The heart was removed and prepared for either dissection of trabecular bundles or for enzymatic digestion. We evaluated the role of KB-R7943 on contractility by assessing isometric force production of isolated atrial and ventricular muscle preparations, and by assessing the percentage shortening of freshly isolated atrial and ventricular myocytes responding to field stimulation. The contribution of revNCX to the Ca2+-transient was assessed using whole-cell voltage-clamp and Fura-2 fluorescence measurements.

In ventricular myocytes, KB-R7943 significantly reduce cell shortening (by 40% from control, n=7, Mann-Whitney Rank Sum, P<0.05) at a concentration of 0.3 μM. The decrease in shortening was greater (by 75% from control, n=6, Mann-Whitney Rank Sum, P<0.05) at a concentration of 5 μM. This reduction is probably due to a decrease in intracellular Ca2+ concentration as our preliminary data shows 5 μM KB-R7943 reduces the amplitude of the Ca2+-transient by approximately 50 %. The reduction in contractility in response to treatment with KB-R7943 was greater in atrial than ventricular cells such that 5 μM KB-7943 completely abolished contraction (n=3).

The relative importance of revNCX decreased as contraction frequency was increased (from 0.2 to 0.8 Hz) in both atrial and ventricular cells. We attribute this to a frequency-induced shortening of action potential duration which reduces opportunity for Ca2+ to enter the cell on revNCX (see Birkedal & Shiels, 2007). In isolated muscle preparations, application of 5 μM KB-R7943 had no effect on peak isometric tension in either atrial (n=7, Mann-Whitney Rank Sum, P<0.05) or ventricular (n=6, Mann-Whitney Rank Sum, P<0.05) muscle over the entire range of contractile frequencies examined (0.2 – 2.0 Hz). This dose may be too low for trabecular muscle preparations.

We conclude that revNCX is an important Ca2+ influx pathway in trout myocytes and is relative importance is affected by the frequency of contraction.

Birkedal R & Shiels H (2007). Am J Physiol. 293, 861-866.

Hove-Madsen L, Llach A, & Tort L (2000). Am J Physiol 279, 1856-64.

Vornanen M, Shiels HA, & Farrell AP (2002). Comp Biochem Physiol A 132, 827-846.

This work was supported by the BBSRC and The University of Manchester.

Authors have confirmed where relevant, that experiments on animals and man were conducted in accordance with national and/or local ethical requirements.

PC17

Caveolar remodelling in rabbit left ventricular myocytes after cell isolation

R.A. Burton[1], G.K. Picton[1], M. Fink[1], P. Camelliti[1], T. Mansoori[2], C. Bollensdorff[1], J. Sheldon[3], G. Bub[1] and P. Kohl[1]

[1]Physiology, Anatomy, Genetics, University of Oxford, Oxford, Oxfordshire, UK, [2]Computing Laboratory, University of Oxford, Oxford, Oxfordshire, UK and [3]Biological & Molecular Sciences, Oxford Brookes University, Oxford, Oxfordshire, UK

Introduction: Caveolae (CAV) are centres of cardiac signal transduction, often studied in isolated cardiomyocytes (M). Little is known about CAV preservation in isolated M, so we monitored this for up to 8h after cell isolation.

Methods: Left ventricular M were isolated from New Zealand (NZ) white rabbit (<1kg) after Schedule 1 killing (conforming to UK Home Office regulations). After excision, the heart was swiftly connected to a Langendorff system, perfused with physiological saline, then cardioplegically arrested (high K+), followed by enzymatic digestion (L-type collagenase; Sigma-Aldrich). Isolated M were stored in saline with BSA and trypsin inhibitor at 22°C (pH 7.4) until fixation with Karnovsky's formaldehyde-glutaraldehyde mix at 0h, 3h or 8h after isolation. M were resin embedded, sectioned longitudinally (80nm), and imaged by transmission electron microscopy. CAV in direct contact or 'within reach' of the sarcolemma (CAVs; centre <50nm from sarcolemma) were distinguished from internal ones (CAVi). For each M, CAVs and CAVi were quantified within a 1μm sub-sarcolemmal space of 9-12 sarcomeres (6 M at each time point). Kruskal-Wallis and Ranksum tests were used (p<0.05).

Results: The density of CAVi and CAVs decreases with time after isolation (Fig.1). The proportion of CAVs increases from 66% at 0h (70% at 3h) to 80% at 8h. At 0h, no CAVs were in a 'semi-open state', i.e. with wide connection between CAV lumen and

extracellular space, while this sub-group increased at later time points (36% of CAVs at 3h, 42% of CAVs at 8h).
Discussion: Isolated M experience CAV loss. This may be caused by either (or both) internalization of CAVs and degradation of CAVi, or progressive sarcolemmal incorporation of CAVs replenished by CAVi. Sarcolemmal integration of CAVs ('semi-open fraction') has been seen during stretch and swelling of Langendorff-perfused rabbit hearts (Kohl *et al*. 2003). This, and more recent observations on stretch-induced redistribution of CAV proteins into the sarcolemma (Calaghan & White 2008), suggests that mechanical factors contribute to CAV destabilization. Cell isolation and storage may provide such mechanical clues (cell swelling in saline). Membrane-integration of CAV can have potentially relevant effects, from increased sarcolemmal surface area and loss of CAV 'lumen', to exposure of proteins to novel environments and destruction of functional microdomains.
Conclusion: Significant remodelling of CAV occurs in M within a time relevant for single cell research.

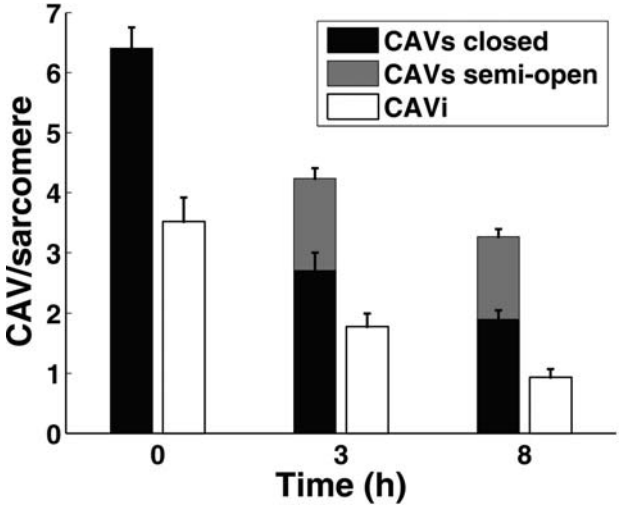

Fig. 1: Decline in CAV numbers per sarcomere (in 1μm sub-sarcolemmal space) with time after cell isolation.

Kohl et al. 2003, PBMB, 82, 221-227.

Calaghan & White, 2008, Biophys J, January suppl, 126a.

Authors have confirmed where relevant, that experiments on animals and man were conducted in accordance with national and/or local ethical requirements.

PC18

3D reconstruction of microtubules, sarcoplasmic reticulum, and T-tubular membrane interrelation in rat ventricular myocytes using electron tomography

P. Camelliti[1], F. Mason[1], M.K. Morphew[2], A. Hoenger[2] and P. Kohl[1]

[1]Department of Physiology, Anatomy & Genetics, University of Oxford, Oxford, UK and [2]Department of Molecular, Cellular & Developmental Biology, University of Colorado, Boulder, CO, USA

Stretch of single cardiomyocytes acutely raises Ca^{2+} spark rate via a microtubule mediated mechanism of unknown nature [1,2]. Prior confocal and immuno-gold transmission electron microscopy suggested that microtubules co-localise with sarcoplasmic reticulum ryanodine receptors [3]. However, antibody-dependence and 2D nature of these techniques makes quantitative assessment of co-localisation difficult. Here, we use electron tomography (5 nm resolution) [4] to study the 3D spatial interrelation of microtubules, sarcoplasmic reticulum, and T-tubular system.
Adult rat ventricular myocytes were chemically fixed, post-fixed in OsO_4, dehydrated and embedded in resin. Sections (250 nm) were imaged with a 300kV electron microscope (Tecnai F30). Dual-axis tilt-series (1° steps, ±60° per axis) were acquired, aligned and combined to reconstruct 3D volumes (tomograms) from five different cells. Tomograms were then processed to generate 3D models used to quantify spatial relationship of microtubules, sarcoplasmic reticulum and T-tubular membranes (Figure 1).
Microtubules (tubular structures with a diameter of 24 nm) regularly traverse the sarcoplasmic reticulum—T-tubular membrane complex which contains the cytoplasmic domain of ryanodine receptors. Microtubules approach sarcoplasmic reticulum and T-tubular membranes to within 7 nm and 13 nm, respectively, suggesting spatial proximity that is close enough to support mechanical interaction.
Thus, electron tomography allows quantitative assessment of the 3D interrelation of microtubules, sarcoplasmic reticulum and T-tubules in adult rat ventricular cardiomyocytes. Microtubules are found in very close proximity to sarcoplasmic reticulum and T-tubular membranes, potentially supporting mechanical transmission of information from the extracellular environment to the sarcoplasmic reticulum—T-tubular complex. Thus, microtubules could contribute to the acute mechanical modulation of cellular Ca^{2+} handling.

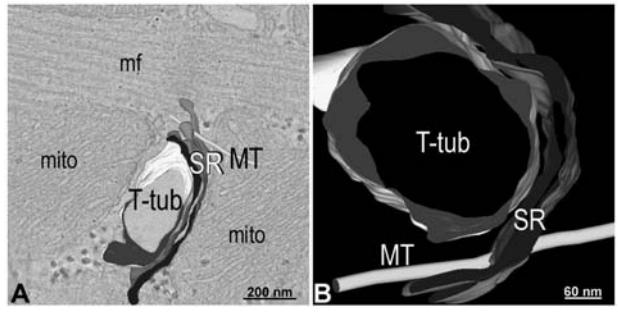

Figure: 1: A) Electron tomogram section and 3D model of a microtubule (MT) near sarcoplasmic reticulum (SR) and T-tubular (T-tub) membranes. B) Zoomed and rotated model showing details of spatial interrelation. mito: mitochondria; mf: myofilaments.

Iribe G et al. (2006). Heart Rhythm 3(5), S47.

Iribe G & Kohl P. (2008). Progress in Biophysics and Molecular Biology (in press).

Camelliti P et al. (2007). Heart Rhythm 4(5), S154-55.

McIntosh R et al. (2005). Trends in Cell Biology 15, 43-51.

We thank Joshua Lynch and Derek Zachman (Department Physiology, University of Colorado, Boulder, CO, USA) for access to isolated myocytes. PC holds a Junior Research Fellowship of Christ Church Oxford, PK is a Senior Research Fellow of the British Heart Foundation.

Authors have confirmed where relevant, that experiments on animals and man were conducted in accordance with national and/or local ethical requirements.

PC19

Alternans of systolic $[Ca^{2+}]_i$ and action potential duration in ventricular myocytes from failing sheep hearts

Y. Li, H.K. Graham, K.M. Dibb, S.J. Briston, M.A. Richards, S.C. O'Neill, L. Miller, A.W. Trafford and D.A. Eisner

Unit of Cardiac Physiology, University of Manchester, Manchester, UK

In previous work we have shown that depressing Ca^{2+}-induced Ca^{2+} release either directly by applying tetracaine (Díaz et al., 2002) or indirectly by decreasing the size of the activating L-type Ca^{2+} current (Díaz et al., 2004) results in a beat to beat alternation of the amplitude of the systolic Ca^{2+} transient. Under these conditions, the larger Ca^{2+} transients resulted from initial unsynchronized release of Ca^{2+} from the sarcoplasmic reticulum that then propagated as Ca^{2+} waves throughout the cell. Beat to beat alternation of the amplitude of cardiac contraction and the action potential duration is commonly seen in heart failure (Kodama et al., 2004). It is not, however, known whether unsynchronized Ca^{2+} release or Ca^{2+} waves are relevant under these conditions.

In order to investigate this question we have used a model of heart failure. Under isoflurane inhalational anaesthesia, pacemakers were implanted in sheep and the ventricle was stimulated at 210 beats per minute. Heart failure was apparent after 4 weeks. Left ventricular midmyocardial myocytes were isolated and loaded with the fluorescent indicator fluo-3. $[Ca^{2+}]_i$ was measured using confocal linescans. Action potentials were stimulated by depolarizing current pulses at 0.5 Hz using the perforated patch technique at room temperature. In 5 out of 20 cells alternation of the action potential duration (measured at 90% repolarization) was seen with the longer action potentials being 111 ± 3 % of the shorter ones. Unsynchronized Ca^{2+} release and resulting Ca^{2+} waves were seen in all these 5 cells. The amplitude of the $[Ca^{2+}]_i$ alternated on a beat to beat basis with different regions of the same cell alternating out of phase.
We conclude that alternans produced by heart failure shows similar changes of Ca^{2+} handling to those observed when Ca^{2+} induced Ca^{2+} release is depressed.

Díaz et al.(2002), Circ Res.91:585-93.

Díaz et al.(2004), Circ Res.94:650-6.

Kodama et al.(2004), J Cardiovasc Electrophysiol.15:295-9.

This work is funded by British Heart Foundation.

Authors have confirmed where relevant, that experiments on animals and man were conducted in accordance with national and/or local ethical requirements.

PC20

Regional differences in preload-dependent modulation of mechanical parameters of Guinea pig single cardiac myocytes

C. Bollensdorff[1], O. Lookin[2], G. Iribe[3] and P. Kohl[1]

[1]Department of Physiology, Anatomy and Genetics, Oxford University, Oxford, UK, [2]Ural Branch of Russian Academy of Sciences, Ekaterinburg, Russian Federation and [3]Okayama University, Cardiovascular Physiology, Okayama, Japan

The Frank-Starling response (preload-dependent modulation of contractility) can be observed in intact isolated cardiomyocytes, but little is known about regional differences in this behaviour. Here, we use a modified version [1] of the carbon fibre (CF) technique [2] to characterize mechanical parameters of cells, isolated from different regions of the Guinea pig heart, during different preloaded conditions.
After Schedule 1 killing (according to UK Home Office guidance), hearts were extracted from female Guinea pigs and Langendorff-perfused with normal Tyrode solution. The tissue was enzymatically digested as described before [1], and cells were harvested separately from the atrium (A), left ventricle (LV) and right ventricle (RV). For experiments, cells were placed in a temperature controlled (37ºC) laminar flow chamber on an inverted microscope stage and stimulated at 2 Hz. CF were attached to cell ends, cells lifted off the coverslip, and CF distance was monitored by online video microscopy (IonOptix; [1]). To increase preload, cells were stretched by up to 30% of slack length (L0). Active and passive force were calculated from observed bending of calibrated CF. End-systolic and end-diastolic lengths and forces (EDL, ESL, EDF, ESF; respectively), amplitude of shortening (dL), maximal velocities of shortening (Vmax_C) and relaxation (Vmax_R), time-to-peak contraction (TTP), and time to 30% relaxation (T30) were identified for each single twitch. To correct for different cell dimensions, cross-sectional area was used to normalize force-related data, while length-related changes were additionally normalized to L0. The normalized data were used to plot x/y parameter relations, and slopes were approximated by linear regression analysis. Slopes were statistically compared for cells from different regions using ANOVA; all data presented as mean±SEM ($p<0.05$).
Changes in EDL had more pronounced effects on dL in A myocytes (10.4±1.16μm/μm) compared to RV (8.7±0.62μm/μm) and LV (9.3±0.41μm/μm). At the same time, EDF rose nearly twice as fast with EDL in A (54.8±1.5mN/mm2) cells, compared to RV and LV (both < 30mN/mm2). The stretch induced gain in Vmax_C and Vmax_R was also significantly higher in A than in LV and RV. At the same time, TTP of A (63.3±9.37ms) cells was significantly lower than in RV (98.3±9.2ms) or LV (99.9±6.7ms). Myocytes from A had significant smaller cross sectional areas and L0 compared to RV and LV. In summary, cardiomyocytes from A are smaller, but show more pronounced contractile responses to increased EDL. This may be of functional relevance for contractile performance of the relatively thin-walled atrium.

Iribe et al. AJP 2007/292:1487-97.

Le Guennec et al. JMCC 1990/22:1083-93.

Supported by the British Heart Foundation.

Authors have confirmed where relevant, that experiments on animals and man were conducted in accordance with national and/or local ethical requirements.

PC21

Deficiency of protein 4.1R in transgenic mice affects cardiac repolarisation and calcium handling

M.A. Stagg[1], U. Siedlecka[1], G.K. Soppa[1], F. Mead[1], A. Baines[2], P. Bennett[3], M.H. Yacoub[1], J.C. Pinder[3] and C. Terracciano[1]

[1]Heart Science Centre, Imperial College London, London, UK, [2]Department of Biosciences, University of Kent, Canterbury, UK and [3]Randall Division of Cell and Molecular Biophysics, King's College London, London, UK

The 4.1 proteins are a family of multifunctional adaptor proteins part of the spectrin-associated cytoskeleton. They promote the mechanical stability of plasma membranes by interaction with spectrin and actin, and they are required for the cell surface expression of a number of ion transporters (Bennett & Baines, 2001). Protein 4.1R is expressed in the heart and upregulated in deteriorating human heart failure but its functional role in the myocardium is unknown. To investigate the role of protein 4.1R on myocardial contractility and electrophysiology, we studied 4.1R-deficient mice (4.1R KO) (Shi *et al.*, 1999). All procedures were performed according to the UK Animals (Scientific Procedures) Act 1986. ECG were measured using radiotelemetry. For the implantation of ECG transmitters the animals were anesthetised by 1.5% isoflurane in 100% oxygen. ECG recording, performed 1 week after surgery, showed that heart rate was reduced (R-R interval (ms): wild type (WT) = 113 ± 5 (6) mean ± SEM (n); 4.1R KO = 139 ± 6 (6); unpaired t test: $p < 0.01$) with prolonged Q-T interval in 4.1R KO (QTc (ms): WT = 46 ± 2 (6); 4.1R KO = 52 ± 1 (6); $p<0.05$). No changes in ejection fraction and fractional shortening, assessed by echocardiography, were found. The action potential duration (APD) in isolated ventricular myocytes was prolonged in 4.1R KO (APD_{75} at 5 Hz (ms): WT = 57 ± 7 (20); 4.1R KO = 81 ± 7 (19); $p<0.05$). Ca^{2+} transients were larger (indo-1 ratio: WT = 0.072 ± 0.01 (22); 4.1R KO = 0.096 ± 0.01 (33); p=0.01) and slower to decay in 4.1R KO (time-to-50% decline (ms): WT = 78 ± 3 (22); 4.1R KO = 91 ± 3 (33); p=0.01). The sarcoplasmic reticulum (SR) Ca^{2+} content (assessed by the application of 20 mM caffeine), and Ca^{2+} sparks frequency were increased (caffeine-induced indo-1 transient (ratio units): WT = 0.09 ± 0.01 (7); 4.1R KO = 0.12 ± 0.01 (16); $p<0.05$); sparks frequency (events/μm/s): WT = 0.52 ± 0.08 (111); 4.1R KO = 1.21 ± 0.1 (124); $p<0.001$). The Na^+/Ca^{2+} exchanger current density was reduced in 4.1R KO (Ni^{2+}-sensitive current at + 80 mV (pA/pF): WT = 3.37 ± 0.1 (14); 4.1R KO = 2.05 ± 0.2 (16); $p<0.05$). The transient inward current inactivation was faster (I_{to} fast time constant (ms): WT = 71 ± 10 (34); 4.1R KO = 40 ± 6 (32); $p<0.05$) and the persistent Na^+ current density was increased in 4.1R KO (integral of 30 μM tetradotoxin-sensitive current at -20 mV measured between 50-300ms from onset (pC/pF): WT = -57 ± 9 (16); 4.1R KO = -98 ± 9 (25); $p<0.01$), with possible effects on APD. Our data indicate that the cytoskeletal protein 4.1R modulates the functional properties of several cardiac ion transporters with consequences on cardiac electrophysiology and with possible significant roles during normal cardiac function and disease.

Bennett DL & Baines A (2001). *Physiol Rev*. **81**, 1353-1392.

Shi Z *et al.*,(1999). *J Clin Invest*. **103**, 331-340.

We thank the Magdi Yacoub Institute for financial support.

Authors have confirmed where relevant, that experiments on animals and man were conducted in accordance with national and/or local ethical requirements.

PC22

Altered gene expression in ventricular tissue induced by sepsis

D.J. Duncan[1], C.M. McGown[2], Z.L. Brookes[2], P.M. Hopkins[3] and S.M. Harrison[1]

[1]Institute of Membrane and Systems Biology, University of Leeds, Leeds, UK, [2]Academic Anaesthesia Unit and Microcirculation Research Group, Royal Hallamshire Hospital, University of Sheffield, Sheffield, UK and [3]Academic Unit of Anaesthesia, University of Leeds, Leeds, UK

Cardiovascular depression occurs during the progression of sepsis leading to tissue hypoperfusion, evident in severe cases. Cellular Ca^{2+} dysregulation, which would contribute to decreased cardiac output, has been reported in whole animal models of sepsis (Zhu *et al*., 2005) and in cellular models where ventricular myocytes are exposed to pro-inflammatory cytokines such as tumour necrosis factor alpha (TNF-α) and interleukin 1β (IL-1β; Duncan *et al*. 2007). In this study, we investigated changes in gene expression induced in ventricular tissue in a whole animal model of sepsis to assess whether targets involved in excitation-contraction coupling were altered.

To model sepsis, male Wistar rats were continuously infused with lipopolysaccharide (LPS, 150 μg/kg/hr) for 24 hr (Gardiner *et al*. 1995) after which they were anesthetised with halothane and killed humanely by cervical dislocation. The heart was then removed and snap frozen. Cross sections of the whole heart weighing ~ 10 mg were dissected and used for RNA extraction. RT-PCR was performed using TaqMan low-density arrays, data normalised to 18S expression and statistical comparisons made between control and septic transcript levels (t-test).

Forty-three transcripts from control (n = 6) and septic (n = 7) hearts were analysed; twenty of the transcripts investigated showed no significant difference between control and septic conditions. These included GAPDH, L-type Ca^{2+} channel, Na^+ channel Nav 1.5 and caveolin. Ten of the 43 transcripts had significantly higher mean mRNA expression ($P< 0.05$ control *vs* septic); expression of inflammatory markers such as TNF-α ($P = 0.005$) and its type 1 receptor ($P = 0.001$) were elevated significantly in sepsis, as was IL-1β ($P = 0.001$) and the nuclear factor kappa light chain gene enhancer ($P = 0.022$).

Thirteen of the 43 targets had significantly lower mean mRNA expression in tissue from septic animals. These included a variety of targets involved in Ca^{2+} regulation; for example SERCA2 ($P = 0.008$), calsequestrin ($P = 0.017$), Na^+/Ca^{2+} exchange ($P =$

0.004) and the Na^+/K^+-ATPase alpha 2 subunit ($P = 0.01$) were all reduced significantly. Interestingly we also observed that a variety of voltage gated K^+ channel genes were down regulated including Kv4.2 ($P = 0.035$), Kv4.3 ($P = 0.002$), HERG ($P = 0.002$), and Kir2.1 ($P = 0.018$).

In summary, changes in gene expression occur during the development of sepsis and include targets that are pivotal in regulating cytosolic Ca^{2+} as well as electrical behaviour. If these changes lead to modified protein expression this would contribute to altered excitation-contraction coupling during sepsis.

Duncan DJ *et al.* (2007). *Br J Pharmacol* **150**, 720-726.

Gardiner SM *et al.* (1995). *Br J Pharmacol* **116**, 2005-2016.

Zhu X *et al.* (2005). *Crit Care Med* **33**, 598-604.

The support of the British Heart Foundation and the Association of Anaesthetists is gratefully acknowledged.

Authors have confirmed where relevant, that experiments on animals and man were conducted in accordance with national and/or local ethical requirements.

PC23

Modulation of atrioventricular nodal cellular electrophysiology by endothelin-1

H. Cheng, C.H. Orchard, A.F. James and J.C. Hancox

Physiology and Pharmacology, University of Bristol, Bristol, UK

Although receptors for the peptide hormone endothelin-1 (ET-1) are densely expressed in the human atrioventricular node (AVN)(Molenaar et al., 1993), there is little if any information at present regarding direct actions of ET-1 on AVN electrophysiology. The aim of the present study was to investigate the effects of ET-1 on spontaneous action potentials (APs) and ionic currents from myocytes isolated from rabbit AVN. Adult male New Zealand White rabbits were killed in accordance with UK Home Office legislation and AVN cells were isolated as described previously (Hancox et al., 1993). Spontaneous APs were recorded continuously with the gap-free acquisition mode by current clamping with a zero-current input. Membrane currents were recorded in whole-cell voltage clamp mode, with a holding potential of -40 mV to 500 ms test pulses applied to a range between -120 and +50 mV at 5 s intervals(Cheng et al., 2007). All recordings were performed at 37 °C. Data were analysed by paired Students' t-test and a $p<0.05$ was considered significant. The rapid application of 10 nM ET-1 led to marked slowing of spontaneous AP rate by 47.3±5.7% (mean±SEM, n=10 cells, $p<0.01$). This concentration of ET-1 also hyperpolarised maximum diastolic potential by -10.3±2.0 mV (n=10, $p<0.01$). The amplitude of peak I_{Ca} at 0 mV was attenuated by 32.7±4.3% (n=10, $p<0.01$). Hyperpolarisation-activated current I_f at –120 mV was unaffected by ET-1 (n= 4, $p>0.05$). Subtraction of the quasi-steady-state (end-pulse) current in control from that in the presence of ET-1 showed that 10 nM ET-1 also activated an inwardly rectifying current that reversed at ~ -85 mV and was outwardly directed at potentials relevant to the diastolic potential range (n=8). To our best knowledge these data represent the first evidence for direct modulation of AVN cell electrophysiology by ET-1.

Cheng H, Orchard CH, Smith GL & Hancox JC. (2007). Acidosis inhibits I_{Ca} and I_{Kr}, but not I_f, in myocytes isolated from the rabbit atrioventricular node. Proc Life Sciences, PC188 (Abstract).

Hancox JC, Levi AJ, Lee CO & Heap P. (1993). A method for isolating rabbit atrioventricular node myocytes which retain normal morphology and function. Am J Physiol 265, H755-766.

Molenaar P, O'Reilly G, Sharkey A, Kuc RE, Harding DP, Plumpton C, Gresham GA & Davenport AP. (1993). Characterization and localization of endothelin receptor subtypes in the human atrioventricular conducting system and myocardium. Circ Res 72, 526-538.

The authors thank Dr. Rachael Baylie for her help in cell isolation and acknowledge support from the British Heart Foundation.

Authors have confirmed where relevant, that experiments on animals and man were conducted in accordance with national and/or local ethical requirements.

PC24

Simulation of atrioventricular nodal reentry using detailed anatomical and action potential models

S. Inada[1], J. Li[1], H. Dobrzynski[1], I.D. Greener[1], J.C. Hancox[2], H. Zhang[1] and M. Boyett[1]

[1]University of Manchester, Manchester, UK and [2]University of Bristol, Bristol, UK

We have investigated the mechanism underlying atrioventricular (AV) nodal reentry using computer simulation. Based on histology and immunohistochemistry, we developed an anatomical model of the rabbit AV node (array of 45,694 nodes) including atrial muscle, transitional tissue, inferior nodal extension, penetrating bundle and ventricular muscle. We assumed (i) the transitional tissue and inferior nodal extension form the fast and slow pathways, respectively, and (ii) the fast pathway, slow pathway and penetrating bundle are composed of atrio-nodal (AN), nodal (N) and nodal-His (NH) cells, respectively. We used a modified version of the Lindblad et al. (1996) model for the rabbit atrial action potential (AP) and we developed biophysically-detailed AP models for rabbit AN, N and NH cells. Stimuli were applied to the atrial septum at a basic cycle length of 350 ms and a S1-S2 protocol was used. Figure 1A shows the activation sequence after the premature (S2) stimulus (S1-S2 interval, 130 ms). The APs did not enter the penetrating bundle through the fast pathway (it was refractory), but it did enter through the slow pathway. From the slow pathway, the AP propagated retrogradely along the fast pathway (as well as anterogradely along penetrating bundle) and reentry occurred. Figure 1B shows selected APs from the atrial muscle, fast pathway, slow pathway and penetrating bundle. After four reentry beats, reentry self-terminated. We have developed an anatomically- and biophysically-detailed model of the AV node, which can be used as a tool to analyse the complex structure and behaviour of the AV node.

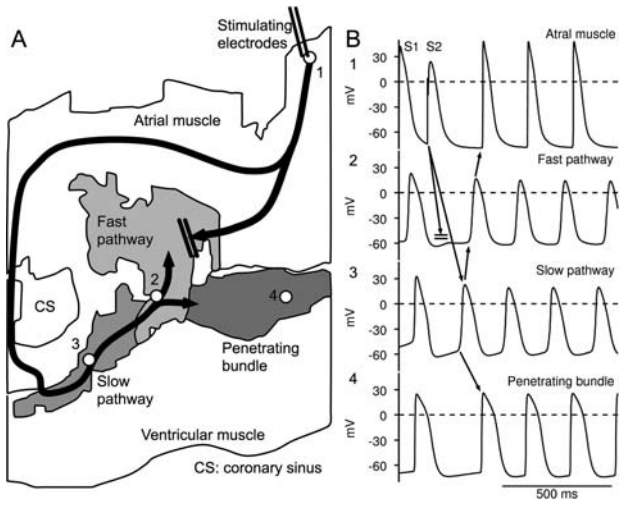

Figure 1
Lindblad D *et al*. (1996). Am J Physiol **271**, H1666-H1696.

Authors have confirmed where relevant, that experiments on animals and man were conducted in accordance with national and/or local ethical requirements.

PC25

K201 maintains cardiac function during Ca^{2+} overload in an isolated working rabbit heart

A. Kelly[1], T. Matsuda[3], A. Rankin[2], R. Matsuda[3], N. Kaneko[3], G.L. Smith[2] and C.M. Loughrey[1]

[1]Faculty of Veterinary Medicine, University of Glasgow, Glasgow, UK, [2]Faculty of Biomedical and Life Sciences, University of Glasgow, Glasgow, UK and [3]School of Medicine, Dokkyo Medical University, Tochigi, Japan

Spontaneous Ca^{2+} release from the sarcoplasmic reticulum (SR) can occur in ventricular cardiomyocytes in situations of high intracellular Ca^{2+} concentrations. Spontaneous SR Ca^{2+} release induced by β-adrenergic stimulation has been linked to contractile dysfunction and potentially lethal arrhythmias[1]. K201 (1,4-benzothiazepine derivative) alters various intracellular Ca^{2+} handling pathways resulting in reduced incidence of spontaneous Ca^{2+} release in cardiomyocytes[2]. While the cardiac-related effects of K201 have been studied using isolated cell preparations the effects on the whole heart remain unclear. Under terminal anaesthesia hearts were removed from adult New Zealand White rabbits and cannulated onto a working heart system. Preload (10cmH2O) and afterload (75cmH2O) were kept constant. Hearts were subjected to increased intracellular Ca^{2+} load by increasing $[Ca^{2+}]_o$ from 2.5mM to 4.5mM, followed 5min later by addition of 150nM isoproterenol (ISO) (n=6) ± 1μM K201 (n=5). In a subset of experiments (n=5) hearts were exposed to increasing concentrations of K201 (0.3, 1 and 3μM) at 2.5mM $[Ca^{2+}]_o$. Mechanical and electrical function was assessed by insertion of a left ventricular 3-French pressure-volume catheter and a bipolar electrogram respectively. Initially, switching to high $[Ca^{2+}]$+ISO significantly increased mean heart rate (HR) (206.9±10.1 vs. 251.7±24.9bpm), developed pressure (DP) (80.4±1.98 vs. 97.4±3.84mmHg) and dP/dt_{max} (1669±109 vs. 3530±183 $mmHg.s^{-1}$; 2.5mM vs. 4.5mM $[Ca^{2+}]$+ISO). After 50s, ectopic electrical events were observed, increasing in frequency from 0.06±0.02 s^{-1} (50s after ISO) to 0.62±0.22 s^{-1} (300s post ISO). HR, DP and dP/dt_{max} decreased (239±16.8bpm, 75.35±5.19mmHg, and 2697±199$mmHg.s^{-1}$) until cessation of aortic flow (AF) 632±70.3s post ISO. In contrast, hearts perfused with K201 maintained AF and mechanical function for a longer period (2545.2±585.25s, ttest P<0.05). HR and coronary flow (CF) were not significantly different between groups. At 2.5mM $[Ca^{2+}]_o$ increasing doses of K201 led to a significant decline in DP [90.5±2.7 (control), 88.1±2.6 (0.3μM), 82.6±2.6 (1μM), 78.7±2.3 (3μM)], and stroke volume (SV) [943±127 (control), 891±131 (0.3μM), 826±120 (1μM), 616±81.3μL (3μM)]. HR decreased significantly in the presence of 1 and 3μM K201 [197.9±5.4 (steady state) 193.6±5.2 (0.3μM), 180.6±4.9 (1μM), 169.8±7.4bpm (3μM)] but not in 0.3μM (197.9±5.4 vs. 193.6±5.2; control vs. 0.3μM K201). Cessation of AF had occurred in all hearts 3min after application of 3μM K201 indicating a narrow therapeutic index. This data demonstrates that perfusion with high $[Ca^{2+}]_o$ and ISO leads to severely impaired contractility and abnormal electrical activity. K201 preserved mechanical function of working hearts during exposure to high$[Ca^{2+}]_o$+ISO, but caused a dose-dependent decrease in mechanical function when perfused with 2.5mM $[Ca^{2+}]$ alone.

Wehrens XH et al (2004). Science 304:292-296

Loughrey CM et al (2007). Cardiovasc Res 76:236-246

Authors have confirmed where relevant, that experiments on animals and man were conducted in accordance with national and/or local ethical requirements.

PC26

Enhanced transmural gradient in I_{to} in a ferret model of heart failure with associated changes in constituent protein expression

L.C. Diffley, K.M. Dibb, H.K. Graham and A.W. Trafford

Cardiac Physiology, University of Manchester, Manchester, UK

The QT interval of the cardiac ECG is frequently increased in heart failure, suggesting ion channel remodelling which has proarrhythmic consequences. The aim of this study was to determine the changes that occur from the in vivo level, down to the level of the ion channel that may contribute to arrhythmogenesis.
Heart failure was induced by aortic coarctation, animals were anaesthetised with an intramuscular injection 70 mg kg^{-1} medetomidine- 7 mg kg^{-1} ketamine. Carprofen analgesic (5 mg kg^{-1}) was administered pre -operatively. Animals were humanely killed with pentobarbitone sodium (200 mg $^{kg-1}$) administered intraperitoneally at the onset of symptoms of heart failure.
The ferret ECG, in lead II configuration, was recorded and analysis of QT interval duration showed 19% increase in the interval in congestive heart failure (CHF) (n=sham, 3; CHF, 4). Action potentials were recorded under current clamp from sham and CHF endocardial and epicardial isolated myocytes and duration measured to 90% repolarisation. An increase in the APD in the

endocardial region of the left ventricle (LV) (P<0.01) correlated with a decrease in I_{to} current density, recorded under whole-cell patch clamp, in the region (P< 0.05; n= sham, 25; CHF, 16). Western blot analysis of the protein constituents of both *Ito* "fast" and "slow" was performed in the sham and CHF ferret tissue. Kv4.2 and Kv4.3 constitute the "fast" component of I_{to} in this model. Analysis of full thickness LV protein preparations revealed that Kv4.2 expression was unchanged but there was an increase in total Kv4.3 in CHF (P=0.03; n= sham, 8; CHF, 8). Western blot analysis was also performed on sham and CHF ferret endocardial and epicardial protein preparations and densitometry analysis revealed down-regulation Kv4.2 in the endocardial region whereas Kv4.3 expression was unchanged (P=0.006; n= sham, 3-4; CHF, 4). Furthermore, there was no change in the expression KChIP2b, the β- subunits to the Kv4 channels in this model. Analysis of transmural Kv1.4 expression, the "slow" component of I_{to} in the ferret, revealed a decrease in expression in the endocardial region of the CHF ferrets relative to sham controls (P=0.03; n= sham, 4; CHF, 4).
In conclusion, the changes in protein expression for Kv4.2, Kv4.3 and Kv1.4 may contribute to the electrical remodelling described above and provide a substrate for arrhythmias in CHF.

This work is supported by the British Heart Foundation.

Authors have confirmed where relevant, that experiments on animals and man were conducted in accordance with national and/or local ethical requirements.

PC26A

Overexpression of SUR2A protects against β-adrenergic-mediated Ca^{2+} loading in cardiomyocytes

R. Sudhir, Q. Du, A. Sukhodub and A. Jovanovic

Maternal and Child Health Sciences, University of Dundee, Dundee, UK

TITLE ONLY

Authors have confirmed where relevant, that experiments on animals and man were conducted in accordance with national and/or local ethical requirements.

PC27

Transcription of the mTOR repressor REDD1 is lower in old women at rest and is downregulated after resistance exercise in young but not old women

C.A. Greig[1], D. Rankin[2], A. Young[1], V. Mann[1], B. Noble[1] and P.J. Atherton[2]

[1]School of Clinical Sciences and Community Health, University of Edinburgh, Edinburgh, UK and [2]School of Graduate Entry Medicine and Health, University of Nottingham, Derby, UK

After a latent period ~1 h post resistance exercise (RE), muscle protein synthesis (MPS) is increased markedly. Previous studies have shown that upregulation of mammalian target of rapamycin complex 1 (mTORC1) signalling is associated with RE-induced MPS through activation of upstream kinases and protein complexes such as Akt, p70S6K1 and TSC1/2, probably through growth factor/mechanosensitive-dependent mechanisms. REgulated in Development and DNA damage responses (REDD1) is a recently identified novel mTORC1 repressor whose transcription is rapidly modulated, and is inversely proportional to mTOR signalling activity (Kimball et al 2008). Thus we hypothesized that REDD1 mRNA expression would be downregulated by exercise as part of the facilitation of mTOR-mediated increases in MPS. We further hypothesized that the downregulation of REDD1 mRNA expression would be greater in young than old women thereby possibly providing a more potent anabolic stimulus in young women.
Twenty two healthy women (old n=9 median age 80 y, range 76-82 y; young n=13, median age 26y, range 19-30 y) undertook a single bout of RE (120 maximal voluntary isometric contractions of the knee extensors of one leg as 20 sets of 6 contractions over 90 minutes). Muscle samples were obtained from the lateral mass of the quadriceps under local anaesthesia (1% lignocaine sc) at baseline and at 2.5 h post-exercise using the Bergstrom needle technique. Changes in muscle mRNA concentration for REDD1 were determined by real-time RT-PCR using pre-validated 28s rRNA to correct for variations in preparation. Statistical analysis was by repeated measures (RM) ANOVA.
In old women at rest muscle REDD1 mRNA was ~30 ± 10 % lower than in muscle of young women (P<0.05) and was unchanged by exercise (Figure 1). In young women, exercise led to an ~80 ± 4 % reduction (P<0.01) in muscle REDD1 mRNA, an expression level that was also significantly lower than that in muscle of old women at rest (P<0.05).
We speculate that the potent downregulation of REDD1 mRNA in young women may be paralleled by a similar decrease in REDD1 protein expression which possibly contributes to increased mTOR signalling and greater initiation of MPS after RE. However, the inability to further respond to RE with downregulation of REDD1 mRNA may limit anabolic responses to RE in old women. Our novel results are consistent with the accumulating evidence for dysregulation of MPS in response to anabolic stimuli in old age.

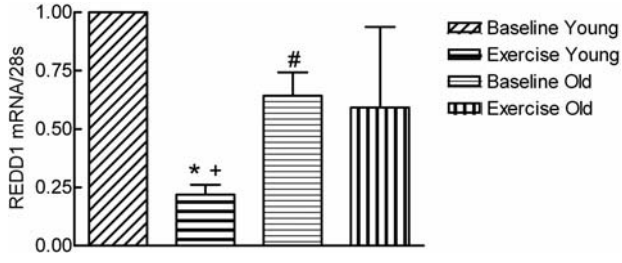

Figure 1: Effect of resistance exercise on mean (SEM) REDD1 mRNA (relative units normalised to baseline for young) for n=9 old and n=10 young women. *+# = P<0.05 (RM ANOVA). * Significantly less than at rest; + significantly less than old women at rest; # significantly less than young women at rest.

Kimball SR, Dang Do AN, Kutzler L, Cavener DR, Jefferson LS, 2008. J Biol Chem 283: 3465-3475.

Funded by Research into Ageing